JACS
JOURNAL OF THE AMERICAN CHEMICAL SOCIETY
Article
pubs.acs.org/JACS

Quantum Chemical Calculations with the Inclusion of Nonspecific and Specific Solvation: Asymmetric Transfer Hydrogenation with Bifunctional Ruthenium Catalysts

Pavel A. Dub and Takao Ikariya*

Department of Applied Chemistry, Graduate School of Science and Engineering, Tokyo Institute of Technology, 2-12-1 O-okayama, Meguro-ku, Tokyo 152-8552, Japan

Supporting Information

ABSTRACT: Details of the mechanism of asymmetric transfer hydrogenation of ketones catalyzed by two chiral bifunctional ruthenium complexes, (*S*)-RuH[(*R*,*R*)-OCH(Ph)CH(Ph)-NH_2](η^6-benzene) (**Ru-1**) or (*S*)-RuH[(*R*,*R*)-*p*-TsNCH(Ph)-CH(Ph)NH_2](η^6-mesitylene) (**Ru-2**), were studied computationally by density functional theory, accounting for the solvation effects by using continuum, discrete, and mixed continuum/discrete solvation models via "solvated supermolecules" approach. In contrast to gas phase quantum chemical calculations, where the reactions were found to proceed via a concerted three-bond asynchronous process through a six-membered pericyclic transition state, incorporation of the implicit and/or explicit solvation into the calculations suggests that the same reactions proceed via two steps in solution: (i) enantio-determining hydride transfer and (ii) proton transfer through the contact ion-pair intermediate, stabilized primarily by ionic hydrogen bonding between the cation and the anion. The calculations suggest that the proton source for neutralizing the chiral RO^- anion may be either the amine group of the cationic Ru complex or, more likely, a protic solvent molecule. In the latter case, the reaction may not necessarily proceed via the 16e amido complex Ru[(*R*,*R*)-XCH(Ph)CH(Ph)NH](η^6-arene). The origin of enantioselectivity is discussed in terms of the newly formulated mechanism.

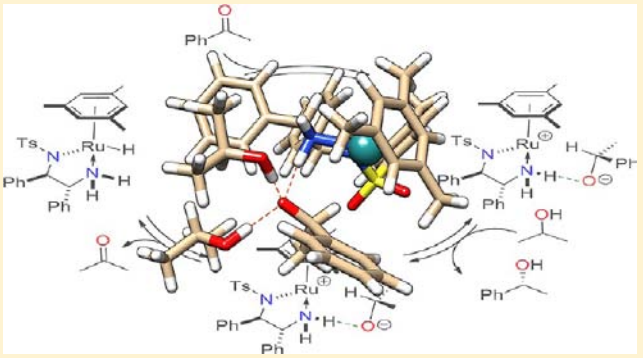

INTRODUCTION

Since the discovery of the conceptually new bifunctional ruthenium catalysts bearing chiral *N*-sulfonylated 1,2-diamine or amino alcohol ligands, RuH[(*R*,*R*)-XCH(Ph)CH(Ph)NH_2]-(η^6-arene) (X = NTs,[1] O[2]), for asymmetric transfer hydrogenation (ATH) of ketones and imines with propan-2-ol or a formic acid/triethylamine mixture, intensive efforts have been made to develop new bifunctional molecular catalysts in both academia and industry.[3] As a result, ATH with well-defined bifunctional catalysts has become one of the most powerful, practical, and versatile tools to access chiral alcohols and amines in organic synthesis because of its excellent selectivity, operationally simplicity, and wide substrate scope.[4] On the basis of mechanistic investigations on the transfer hydrogenation reaction, it has been proposed that a hydride from the ruthenium and a proton from the amine of the 18e ruthenium hydride amine intermediates are delivered to a ketone through a rate-determining six-membered pericyclic[5,6] transition state,[7,8] as shown in Scheme 1.[3,4,9] For the prochiral ketones, this is the enantio-determining step (EDS), during which a chiral product and the 16e amido complex Ru[(*R*,*R*)-XCH(Ph)CH(Ph)NH]-(η^6-arene) are obtained. The proton and the hydride from propan-2-ol are then delivered to the ligand and the metal, respectively, regenerating the hydride and forming acetone. In the case of (*S*)-RuH[(*R*,*R*)-Tsdpen](η^6-*p*-cymene), where Tsdpen = *p*-TsNCH(Ph)CH(Ph)NH_2, both 18e hydride and corresponding 16e amido complexes were isolated and characterized by X-ray studies in the solid state.[10]

The three-bond concerted mechanism via a six-membered pericyclic transition state was experimentally supported by the kinetic isotope effects (KIEs) measurements from Noyori and Ikariya's[10] group and later by Casey's group,[11] who studied reactions between a 16e amido Ru complex Ru[Tsdpen](η^6-*p*-cymene) and propan-2-ol, as well as by quantum chemical calculations from the groups of Noyori,[9d,12] Andersson,[13] van Leewen,[14] Meijer,[15] and Václavík and Kuzma.[16]

It should be noted, however, that a concerted reaction is defined as one that takes place in a single kinetic step.[6,17] Such a classification necessarily depends on the characteristic time of a physical method.[18] Thus, a sufficiently fast nonconcerted reaction that is rapid compared to the applied detection method may be occasionally taken as concerted.[19] The KIE measurements were performed using NMR spectroscopy as a detection method, which is one of the slowest physical methods. Besides, H/D scrambling[20] or quantum tunneling

Received: October 3, 2012
Published: January 21, 2013

dx.doi.org/10.1021/ja3097674 | *J. Am. Chem. Soc.* 2013, 135, 2604−2619

Scheme 1. Interconversion between 18e Amine Hydrido and 16e Amido Ru Complexes via the Proposed Six-Membered Pericyclic Transition State: Plausible Catalytic Cycle for Asymmetric Transfer Hydrogenation of Aromatic Ketones with Propan-2-ol

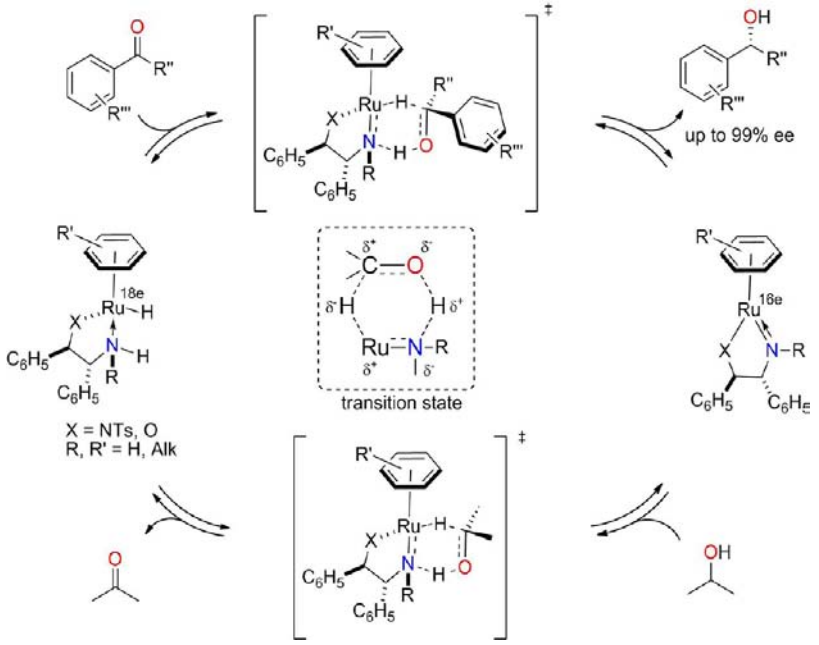

effects[21] could obscure the KIEs. Moreover, all computational studies published so far were performed in the gas phase and did not incorporate the effects of the solvent. Andersson et al. noted[13] that the enantioselectivity of these reactions could be governed by factors not included in the gas phase calculations and that accounting for the solvent effects is necessary for a correct description of this process.[22] The importance of solvation effects and entropy for correct interpretation of the computational data was also highlighted by van Leewen.[14]

Recently, several somewhat conflicting experimental and theoretical studies appeared that do not support the three-bond concerted reaction via a rate-determining six-membered pericyclic transition state in the catalytic transfer hydrogenation reactions catalyzed by bifunctional ruthenium complexes. Xiao and Liu et al. reported a significant acceleration of reaction rates in the ATH of acetophenone with Ru[Tsdpen](η^6-*p*-cymene) catalyst in a binary water/cosolvent mixture.[20] The initial reaction rate and average activity were found to increase with increasing polarity of the cosolvent (hexane < Et_2O < toluene < CH_2Cl_2 < DMF).[20] This observation is not characteristic for the pericyclic reactions,[23] in which the charge distributions in the activated complexes and the reactants are very similar. Rather, it testifies for a dipolar transition-state reaction,[23] where activated complexes differ considerably in charge separation or charge distribution from the initial reactants. Similar results on solvent effects were presented by Tanis et al.,[24] who studied ATH of aryl chloromethyl ketones catalyzed by the Noyori–Ikariya catalyst Ru[(*R*,*R*)-Tsdpen](η^6-*p*-cymene). Bergens and co-workers reported that a Noyori hydrogenation catalyst, *trans*-Ru(H)$_2$[(binap)(dpen)], which is proposed to react with ketones via the same pericyclic transition state,[25] reacted on mixing with acetophenone or other ketones in THF at −80 °C under 2 atm H_2 to generate exclusively the alkoxide *trans*-RuH(OCHPhMe)[(binap)(dpen)].[26] Contrary to expectations from the pericyclic reaction, free amido Ru complex and 1-phenylethanol were not the immediate products of the reaction.[26a,c] To explain the unexpected experimental results, the authors proposed "the formation of a partial Ru−O bond in the concerted transition state". Notably, in the reaction of a related hydrido complex, (*R*)-RuH[(*S*,*S*)-Tsdpen](η^6-*p*-cymene), with acetone in toluene, a 16e amido complex was identified as a kinetic reaction product.[10] In the opposite reaction of the 16e Ru[(*S*,*S*)-Tsdpen](η^6-*p*-cymene) with propan-2-ol or 2,2,2-trifluoroethanol, the hydride[10] or 2,2,2-trifluoroethanoxo[27] complex was identified in the mixture, respectively. Moasser reported that the interaction of acetophenone with the hydrido complex RuH[*N*-(*p*-X-phenyl)-*N*′-(*p*-toluenesulfonyl)-1,2-ethylenediamine](η^6-*p*-cymene) in HCO_2H/NEt_3 mixture via a pericyclic transition state is not plausible, and that CO_2 interacts with the same complex (reverse reaction) possibly via an ion-pair intermediate.[28] An ion-pair intermediate was also proposed in the reaction between Ru[(*R*,*R*)-Tsdpen](η^6-*p*-cymene) and formic acid.[29]

Meijer and co-workers reported *ab initio* molecular dynamics study of the hydrogen transfer reaction between simplified model RuH[$XCH_2CH_2NH_2$](η^6-C_6H_6) (X = O,[30] NH-(SO_2CH_3)[31]) and formaldehyde in a cubic box containing explicit molecules of methanol[30] or water,[31] respectively, based on the discrete solvation model. These two works represent the only available computational studies that deal with solvent effects in the seminal system, and they revealed that (1) "the activation barriers were lowered and the concerted mechanism predicted in the gas phase was converted into a sequential mechanism in methanol solution with the substrate appearing as methoxide-like intermediate, which existed for a short but finite time in the reactive trajectory",[30] and (2) "a concerted transition state was observed in water solution, however, only the hydride was transferred at that point, whereas the proton was transferred later by a water molecule".[31] The authors proposed a "concerted solvent-mediated mechanism of the proton transfer" in methanol solution.[30] Xiao and Liu reported

dx.doi.org/10.1021/ja3097674 | *J. Am. Chem. Soc.* 2013, 135, 2604−2619

that one explicitly hydrogen-bonded water molecule contributes to the asynchronicity of the three-bond concerted reaction between simplified RuH[$NH_2CH_2CH_2NH_2$](η^6-C_6H_6) and acetone via a six-membered pericyclic transition state, based on gas phase DFT/BLYP calculations.[20] They located on the reaction coordinate a first-order saddle-point ($i303$ cm^{-1}) in this "microsolvated" complex that corresponds "mostly to the transfer of the hydride between Ru and the carbonyl C atom". Note that initially an asynchronous or *two-stage*[17a,b] three-bond[17a] concerted reaction via a six-membered pericyclic transition state was originally reported[9d] by Noyori in their gas phase calculations.[32]

Given the importance of ATH reactions with bifunctional complexes in academic and industrial syntheses of chiral compounds, it is desirable to arrive at a full mechanistic understanding of this catalytic reaction, which should also conform to the recently reported experimental[20,24,26a,b,28] and catalytic[20,33] anomalies that do not fit the pericyclic mechanism. In the year 2012, a dozen of scientific contributions on catalytic transfer hydrogenation with bifunctional complexes were published in which the concept of the rate-determining six-membered pericyclic transition state, based on the gas phase model, is used.[33,34] In the present work we probe the influence of the continuum solvent reaction field as well as individual explicit solvent molecules of propan-2-ol on the reactions between unabridged chiral models[35] of the ruthenium hydride complexes (*S*)-RuH[(*R*,*R*)-OCH(Ph)CH(Ph)NH_2](η^6-benzene) (**Ru-1**) and (*S*)-RuH[(*R*,*R*)-*p*-TsNCH(Ph)CH(Ph)-NH_2](η^6-mesitylene) (**Ru-2**) with acetone or acetophenone in the framework of the density functional theory (DFT).[36] We study these reactions using a technique that takes into account *nonspecific* (or *macroscopic*) or *specific* (or *microscopic*) solvation effects or both of propan-2-ol via the "solvated supermolecules" approach, where the Schrödinger equation is solved for the entire solute−solvent complex in the solvent polarization electric field (reaction field).

COMPUTATIONAL DETAILS AND GENERAL METHODOLOGY

All calculations were carried out with the Gaussian 09 software[37] using the Tsubame-2 supercomputer (TokyoTech).[38] The reactions between **Ru-1** and acetone or acetophenone were studied at the DFT/M06/SDD(Ru)/6-311++G**(C,H,N,O) level of theory in the gas phase or in the continuum solvent reaction field of propan-2-ol using the SMD solvation model.[39] The reactions between **Ru-2** and acetone or acetophenone were studied under the same level of theory, but with the 6-31G* basis set for the (C,H,N,O,S)-atom block. The reactions between complexes RuH[$XCH_2CH_2NH_2$](η^6-C_6H_6) [X = O, NH_2] and acetone or formaldehyde were studied with the SDD(Ru)/6-311++G**(C,H,N,O)-basis set with M06[40] or BLYP[41] functionals, in the continuum solvent reaction field using SMD[39] or C-PCM[42] solvation model. DFT integration grids with 99 radial and 590 angular points (Ultrafine) were used for all calculations. For the 6-311++G**(C,H,N,O) frequency calculations of the "solvated supermolecules", integral accuracy was increased to the 1×10^{-11} cutoff by using the option "Int=(Acc2e=11,Grid=Ultrafine)". The molecular cavity was created as implemented in Gaussian 09 via the SMD or C-PCM solvation model. All the calculations were carried out on the conformers of the ruthenium complexes having λ-configured five-membered N−N ring with C−H hydrogen atoms located at the axial positions (Chart S1, Schemes S1 and S2). In the case of (*R*,*R*)-Tsdpen, the absolute configuration on the N(Ts) atom was *R*. This structural arrangement (λ,N_R) was found for the 18e hydrido complex (*S*)-RuH[(*R*,*R*)-Tsdpen](η^6-*p*-cymene) in the solid state (X-ray structure).[10] All geometries were fully optimized without symmetry or geometry constraints. In this work, gas phase optimized geometries are labeled with Roman numerals, and continuum solvent reaction field optimized geometries are labeled with Arabic numerals (Schemes S1 and S2). Frequency calculations were carried out for all optimized geometries under the harmonic approximation. The Gibbs free energies, *G*, were calculated under standard-state conditions as default in Gaussian: T = 298.15 K, p = 1 atm (gas), or C = 1 M (continuum model). Intrinsic reaction coordinate (IRC) calculations[43] were computed for most of the transition states separately in the forward and reverse directions. Molecular graphics images were produced using the UCSF Chimera package.[44] The results are discussed in terms of electronic and free energies, although modern computational modeling cannot accurately handle enthalpies and especially entropies in solution, which is a major computational challenge for which no universal solution is apparently available.[45] Because entropic factors are typically overestimated by the current computational methods (especially for the reactions with a different number of particles on the right and on the left),[46] an accurate Gibbs energy could be estimated to lie between the computed values of the electronic energy (E) and Gibbs energy (G) profiles.[47]

Solvent effects can be grouped into two distinct components.[48] "*Nonspecific*" or "*macrosolvation*" describes the interaction between the solute molecule and the solvent polarization electric field (reaction field) around the solute in the solution. The "*specific*" or "*microsolvation*", the origin of which are hydrogen-bonding forces, charge transfer or electron-pair donor−acceptor complexes, are defined by the formation of kinetically stable complexes between solute and solvent. In quantum chemistry, three general approaches have been used for the theoretical description of solute/solvent interactions:[49] continuum models, discrete solvation models, and mixed continuum/discrete models. The first group of methods[49d,50] treats the solvent as a continuous medium characterized by its macroscopic dielectric constants; thus, it provides the description of the *nonspecific* solvation. Continuum models are particularly efficient tools for studying the effects of condensed phases on molecular structure, energetics, properties, and dynamics when solvents interact only slightly with the solute.[50a,c] In the second group of methods, such as the supermolecular model,[51] frozen density functional approach,[52] *ab initio* molecular dynamics,[53] Monte Carlo,[54] or the combined quantum mechanical and classical mechanical models (QM/MM),[55] one or more solvent molecules are treated explicitly. Importantly, in the continuum model the explicit microscopic structure of the solvent is neglected; therefore, this model provides a poor description of the short-range interactions. As a result, not all of the electronic aspects of hydrogen bonding between solvent and solute are correctly described by continuum models. On the other hand, the explicit descriptions with the discrete model, which are always size-limited, cannot fully take into account long-range (bulk) effects. To take into account both *nonspecific* and *specific* interactions, the "solvated supermolecules" (or mixed continuum/discrete) model was applied.[50c,56] This model uses a generalized continuum model in which the solute contains several explicit solvent molecules belonging to the first solvation shell.[50c] In view of recent developments, we have chosen to use the "solvated supermolecules" approach primarily for modeling the catalytic ATH with bifunctional ruthenium complexes.

RESULTS AND DISCUSSION

Computational quantum chemistry has become a powerful addition to experiment to investigate chemical reactions on the molecular level.[57] Although theoretical chemists have developed a variety of computational strategies for describing and understanding the complex phenomenon of solvation, theoretical modeling of molecular properties in the condensed phase, contrary to the gas phase, is still rather limited, as well as much more difficult and time-consuming. Chemical reactions in solution, however, are dictated mainly by the solvent.[48a] Solute−solvent interactions have dramatic effects on molecular structures, energies, and properties[49e,58] as well as on the

dx.doi.org/10.1021/ja3097674 | J. Am. Chem. Soc. 2013, 135, 2604−2619

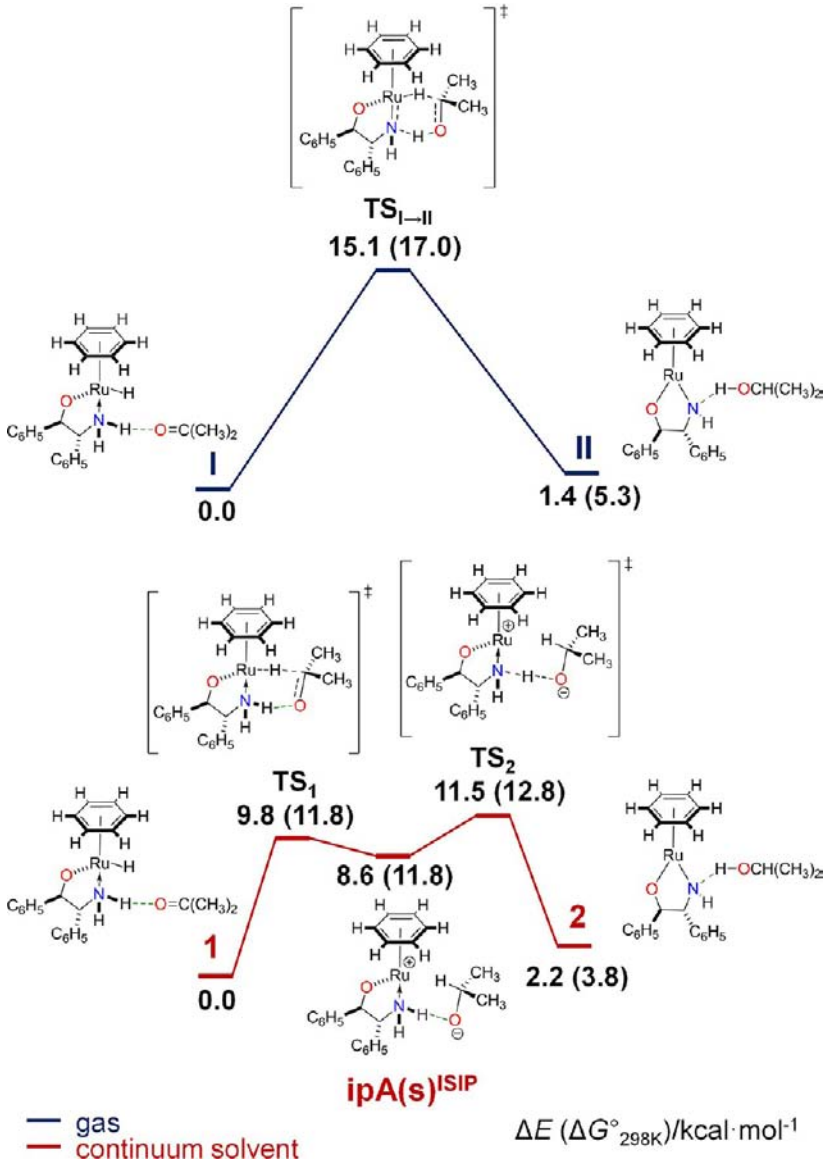

Figure 1. DFT/M06/SDD(Ru)/6-311++G**(C,H,N,O) gas phase vs continuum solvent reaction field energy profiles for the reaction between (*S*)-RuH[(*R*,*R*)-OCH(Ph)CH(Ph)NH$_2$](η^6-C$_6$H$_6$) (**Ru-1**) and acetone. For the continuum solvent reaction field, the SMD (propan-2-ol) solvation model[39] is used.

outcome of the reaction, including the sense of the enantioselection.[33,59] In contrast to the gas phase, where reactions without charge separation or charge distribution are preferred (e.g., radical-producing and pericyclic reactions), in solution preferable reactions are the ones involving charge separation and charge distribution.[48a] In order to introduce solvation effects into the calculations, three solvation models were examined and compared, i.e., continuum, discrete (by introducing up to two solvent molecules around the reacting complex at the hydrogen-bonded positions), and mixed continuum/discrete models, via the "solvated supermolecules" approach. Comparison of the present methods with the CP-MD,[30,31] a method which is based on the dynamic approach is available in the Supporting Information (SI, pp S6−S10).

Reaction of (*S*)-RuH[(*R*,*R*)-OCH(Ph)CH(Ph)NH$_2$](η^6-C$_6$H$_6$) (Ru-1) with Acetone. *Gas Phase vs Continuum Solvent Reaction Field (Gas vs Continuum Solvation Model).* At first the reaction between (*S*)-RuH[(*R*,*R*)-OCH(Ph)CH(Ph)NH$_2$](η^6-C$_6$H$_6$) (**Ru-1**) and acetone was studied in the gas phase. We found, in agreement with previously reported data (*vide supra*), that two oppositely polarized hydrogen atoms, a hydride from the ruthenium center and a proton from the amine, are delivered from the 18e ruthenium hydride complex **Ru-1** to the acetone through the three-bond concerted transition structure **TS$_{I\rightarrow II}$** (*i*1372 cm^{-1}) as shown in Figure 1. In this context and for the purpose of this work, it is not exactly important whether this transition structure is classically pericyclic or pseudopericyclic.[60] Nucleus-independent chemical shift (NICS)[61] calculations (see SI, Figure S4) suggest that the concerted structure is rather classically pericyclic. In this transition structure, all six atoms are located almost in one plane, with a dihedral angle RuNOC of 5°. Analysis of the vibrational vector reveals that two hydrogen atoms are delivered to the acetone molecule slightly asynchronously, i.e., via a three-bond, *two-stage*[17a] concerted process. IRC calculations[43] performed for this transition state, **TS$_{I\rightarrow II}$**, clearly revealed two minima that correspond to the hydrogen-bonded adducts **I** and **II** (see Figure 1). Optimized geometries of **I**,

dx.doi.org/10.1021/ja3097674 | *J. Am. Chem. Soc.* 2013, 135, 2604−2619

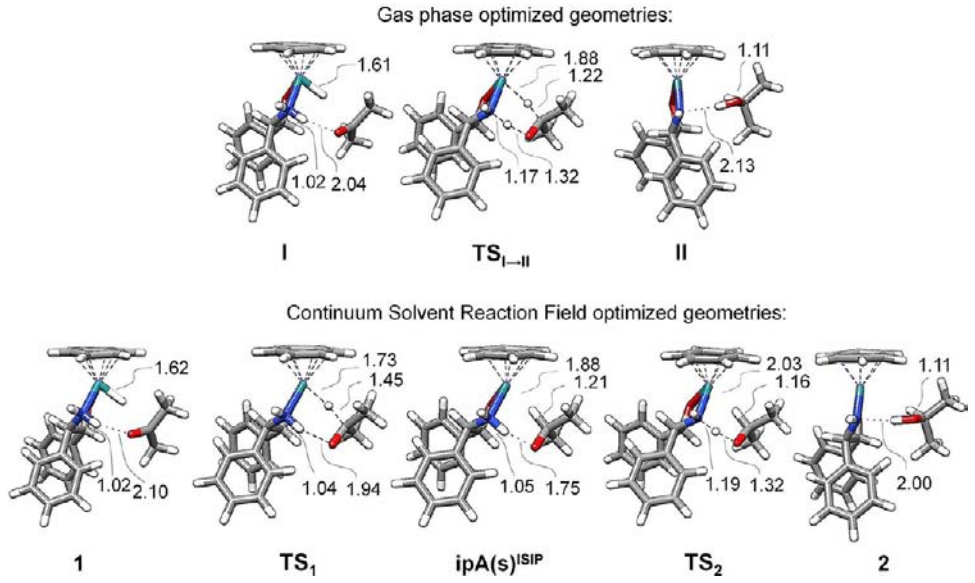

Figure 2. DFT/M06/SDD(Ru)/6-311++G**(C,H,N,O)-optimized geometries of the stationary points along the reaction coordinate between (*S*)-RuH[(*R*,*R*)-OCH(Ph)CH(Ph)NH$_2$](η^6-C$_6$H$_6$) (**Ru-1**) and acetone to afford **II** (**2**) in the gas phase or continuum solvent reaction field of propan-2-ol using the SMD solvation model.[39] Selected bond lengths are presented.

TS$_{I\rightarrow II}$, and **II** as well as selected bond lengths are presented in Figure 2.

Further, the reaction of **Ru-1** with acetone was studied in the continuum solvent reaction field of propan-2-ol using the SMD solvation model.[39] Optimization of **TS$_{I\rightarrow II}$** in the propan-2-ol continuum solvent reaction field afforded the transition structure **TS$_2$** (i1342 cm^{-1}), in which clearly only the proton transfer is taking place, as shown in Figures 1 and 2. IRC calculations of this transition structure revealed two minima that correspond to the ion-pair **ipA(s)^{ISIP}** and hydrogen-bonded adduct **2**, respectively (Figures 1 and 2). Structural, orbital, and natural bond population analyses (see SI, Figures S5, S6, S7) suggest that **ipA(s)^{ISIP}** is an inner-sphere contact ion-pair (ISIP), which is additionally stabilized by the ionic N−H···O$^-$ hydrogen bond between the cation and the anion.[62] The ion-pair **ipA(s)^{ISIP}** has the counterion in the first coordination sphere of the metal-containing moiety and a slightly elongated C−H bond of the anion that is directed toward the Ru atom, as shown in Figure 2. All six atoms occupy almost planar positions, with a dihedral angle RuNOC of 4°. Natural bond orbital (NBO) analysis indicates that the C−H hydrogen atom has a weak interaction with the metal and q_H = 0.086, which can be compared with the hydride charge in **1** (q_H = 0.006) and the proton charge in **2** (q_H = 0.165). The C(H)···Ru distance of 3.06 Å (cf. 3.73 Å, the sum of the van der Waals radii),[63] the elongated C−H distance of 1.21 Å (cf. 1.12 Å in "free" anion), and the almost linear angle C−H$^{\delta+}$···Ru of 163° testify the "non-classical" C−H···Ru hydrogen-bonding interaction.[64] At the same time, the oxygen atom in **ipA(s)^{ISIP}** bears the highest negative charge (q_O = −0.923) along the reaction coordinate, cf. q_O = −0.675 in **1** and q_O = −0.836 in **2** (Figure S7). We further found that complex **1** and **ipA(s)^{ISIP}** are connected via the transition state **TS$_1$** (i333 cm^{-1}), corresponding to pure hydride transfer from Ru to C in the outer sphere, as shown in Figure 1. IRC calculations from this first-order saddle point resulted in **1** and **ipA(s)^{ISIP}** as local minima.

Thus, introduction of only the *nonspecific* solvation of propan-2-ol for the reaction of **Ru-1** with acetone clearly indicates a two-step reaction with the ionic pair **ipA^{ISIP}** as a metastable intermediate.[65] The transition state corresponding to hydride transfer is quasi-pericyclic, since all six atoms lie almost in the plane (dihedral angle RuNOC = 1°) and there is a hydrogen bond between the N−H hydrogen and oxygen O atoms. However, the reaction should be viewed as one-bond concerted,[17a] because the process involves the breaking and forming of only one bond, Ru−H and C−H, respectively. The relative barriers are significantly decreased, by ∼8 kcal/mol, in the solvent reaction field relative to the gas phase. The calculated barrier for the proton transfer is ∼2 kcal/mol higher than the barrier of the hydride transfer on both electronic and free energy scales, as shown in Figure 1. Analysis of **TS$_2$** reveals that a weak C−H···Ru hydrogen bond is still present in the transition state ($d_{Ru\cdots(H)C}$ = 3.10 Å, angle Ru···H−C = 152°); however, all atoms of the six-membered cycle occupy less planar positions, with the dihedral angle RuNOC of 8°, cf. 4° in **ipA(s)^{ISIP}** and 1° in **TS$_1$**. Synchronous breaking of the N−H covalent bond, weak C−H···Ru hydrogen bond, and transformation of the distorted octahedral configuration around the ruthenium center in **ipA(s)^{ISIP}** into a square-planar geometry of **2** possibly make the N−H proton transfer visibly higher in energy than the preceding hydride transfer step. This observation, however, is only valid for a 1:1 reaction in the reaction field. Introduction of explicit solvent molecules into the calculations further stabilizes the proton transfer step (*vide infra*).

Inner-sphere ion-pair **ipA(s)^{ISIP}** is a branching point of the reaction: in addition to the N−H proton transfer from the ruthenium cation to the isopropoxide anion in **ipA(s)^{ISIP}** to afford **2** as described in Figure 1, partial or full dissociation to give different contact ion pairs or "free" ions, respectively, is possible. Corresponding stationary points are described in Figure S9. Of note is the formation of the outer-sphere ion pair[62] **ipA(s)^{OSIP}**, which is also hydrogen-bonded via N−H···$^-$OCH(CH$_3$)$_2$, obtained from **ipA(s)^{ISIP}** via relegation of the isopropoxide anion to the second coordination sphere, as shown in Figure S9. This process is accompanied by partial transformation of the distorted octahedral configuration around

dx.doi.org/10.1021/ja3097674 | *J. Am. Chem. Soc.* 2013, 135, 2604−2619

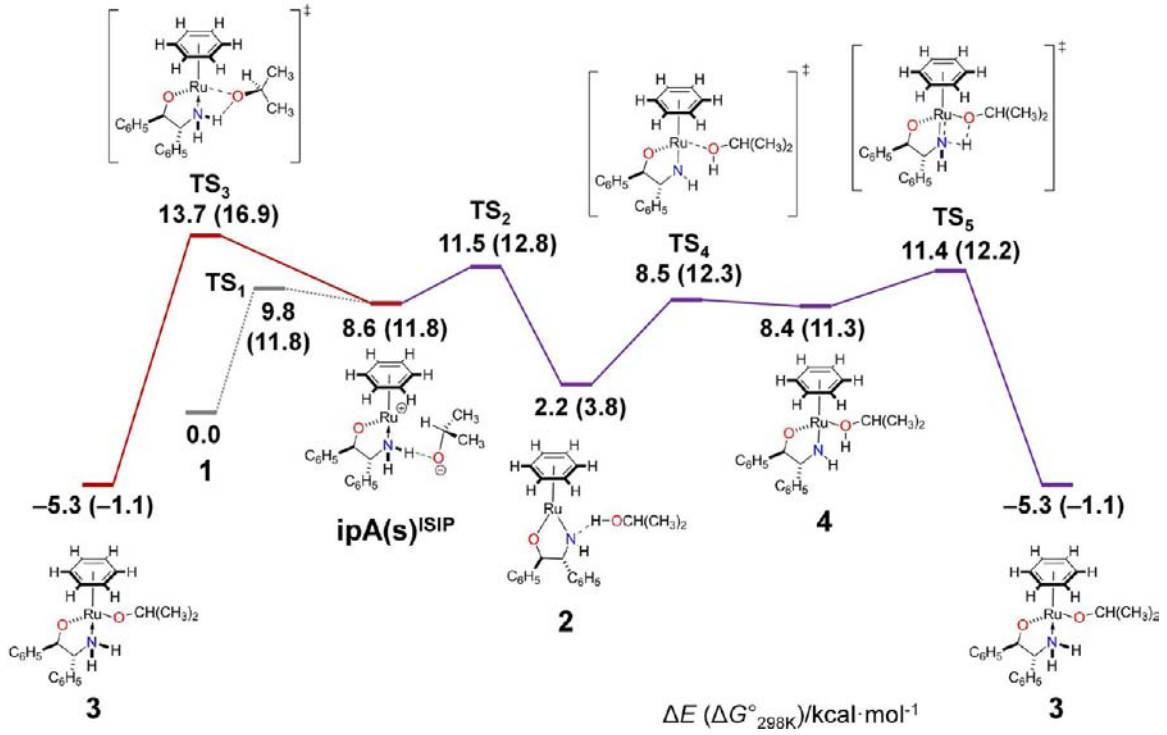

Figure 3. Formation of isopropoxo ruthenium complex (*S*)-Ru(OCH(CH$_3$)$_2$)[(*R*,*R*)-OCH(Ph)CH(Ph)NH$_2$](η^6-C$_6$H$_6$) (**3**) from **ipA(s)**^{ISIP}: directly via anion reorientation (red line), or stepwise via complexes **2** and **4** (violet line). Energy profile at the DFT/M06/SDD(Ru)/6-311++G** (C,H,N,O)/SMD(propan-2-ol) level of theory.

the ruthenium center (angle CNT^{benzene}–Ru–CNT^{NO} = 151°, where CNT denotes a centroid) into a square-planar geometry (angle CNT^{benzene}–Ru–CNT^{NO} = 157°) and significant breaking of the C–H···Ru hydrogen bond ($d_{C(H)\cdots Ru}$ = 3.40 Å, angle C–H···Ru = 141°). In the reaction field, however, **ipA(s)**^{OSIP} is 2.6 kcal/mol higher on the free energy scale. The ion pair **ipA(s)**^{ISIP} could afford directly the ruthenium isopropoxo complex (*S*)-Ru(OCH(CH$_3$)$_2$)[(*R*,*R*)-OCH(Ph)-CH(Ph)NH$_2$](η^6-C$_6$H$_6$) (**3**) via the reorientation and coordination of the anion as shown in Figure 3. This reaction is very favorable thermodynamically, with ΔG°_{298K} = −12.9 kcal/mol. This step is characterized by an activation barrier ($\Delta G^{\ddagger}_{298K}$) of 5.1 kcal/mol. The corresponding transition state **TS$_3$** (*i*74 cm^{-1}), however, is higher by 2.2 kcal/mol on the electronic energy scale or 4.1 kcal/mol on the free energy scale than **TS$_2$** of the proton transfer to afford **2** as shown in Figure 3. Complex **2**, however, is less stable than **3** by 4.9 kcal/mol on the free energy scale.

Analysis of the reverse IRC that connects **TS$_3$** with **ipA(s)**^{ISIP} reveals that this process proceeds via opening of the dihedral angle RuNOC from 4° in **ipA(s)**^{ISIP} to 60° in **TS$_3$**, during which the weak C–H···Ru hydrogen bond is broken. This process occurs in the first coordination sphere of the metal, and the ruthenium center has a distorted octahedral configuration. After the first-order saddle point **TS$_3$** is reached, the following descent line on the potential energy surface (PES) corresponds to oxygen anion coordination on the ruthenium cation to afford **3**. Alternatively, the latter can be obtained from **2** via O–H bond cleavage based on metal–ligand cooperation without a change in the formal oxidation state of the metal (bifunctional activation), as shown in Figure 3. This process occurs via two steps: slightly thermodynamically unfavorable coordination of propan-2-ol on ruthenium (ΔG°_{298K} = 6.2 kcal/mol) via **TS$_4$** (*i*66 cm^{-1}) to afford **4**, during which the square-planar geometry around the initial 16e ruthenium complex is transformed into a distorted octahedral configuration of an 18e complex, and subsequent intramolecular proton transfer through a four-membered, one-bond[17a] concerted reaction, **TS$_5$** (*i*728 cm^{-1}). These steps are characterized by activation barriers ($\Delta G^{\ddagger}_{298K}$) of 8.6 and 0.9 kcal/mol, respectively. Thus, the amido complex **2** is a kinetic reaction product in the reaction between the hydrido complex **1** and acetone, whereas **3** is a thermodynamic reaction product.

Supermolecules vs "Solvated Supermolecules" (Discrete vs Mixed Continuum/Discrete Solvation Model). Amphiprotic solvents, similarly to water, could be viewed as dynamic three-dimensional hydrogen-bonded networks.[48a] Normal hydrogen bonds are approximately 10 times stronger than the nonspecific intermolecular interaction forces;[48a] thus, it was of interest to examine the influence of protic solvent molecules on the reaction of (*S*)-RuH[(*R*,*R*)-OCH(Ph)CH(Ph)NH$_2$](η^6-C$_6$H$_6$) (**Ru-1**) with acetone. In the computational analysis we examined both the gas phase and continuum solvent reaction field for the reactions of **Ru-1** with acetone in the presence of one or two molecules of propan-2-ol, located at hydrogen-bonded positions around the reacting complex between **Ru-1** and acetone, as shown in Figures 4 and 5. In both the gas phase and continuum solvent reaction field with one or two explicit solvent molecules, similar two-step profiles were obtained, as shown in Figure 4. The first step consists of hydride transfer from **Ru-1** to acetone through H-bonded adducts to afford ISIP intermediates via the transition states **TS$_{V\rightarrow ipB}$**^{ISIP} (one solvent molecule in the gas), **TS$_{VII\rightarrow ipC}$**^{ISIP} (two solvent molecules in the gas), **TS$_6$** (one solvent molecule in the reaction field), and **TS$_8$** (two solvent molecules in the reaction field). The second step consists of proton transfer from the nitrogen atom to the

dx.doi.org/10.1021/ja3097674 | *J. Am. Chem. Soc.* 2013, 135, 2604–2619

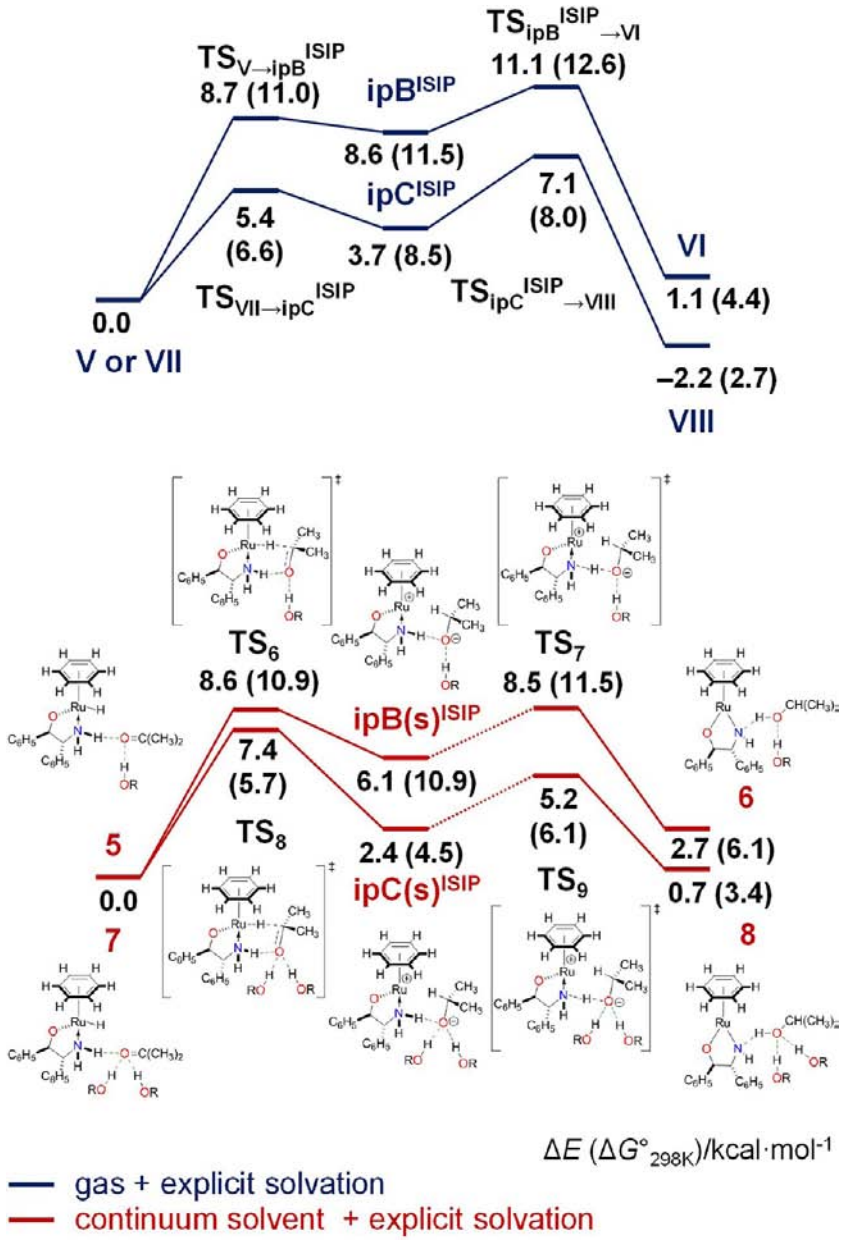

Figure 4. DFT/M06/SDD(Ru)/6-311++G**(C,H,N,O) gas phase vs continuum solvent reaction field energy profiles of the reaction between (*S*)-RuH[(*R*,*R*)-OCH(Ph)CH(Ph)NH$_2$](η^6-C$_6$H$_6$) (**Ru-1**) and acetone in the presence of one or two explicit propan-2-ol molecules. For the continuum solvent reaction field the SMD (propan-2-ol) solvation model[39] is used. R = CH(CH$_3$)$_2$.

oxygen anion to afford the hydrogen-bonded 16e Ru complexes with two or three molecules of propan-2-ol via **TS$_{ipB}^{ISIP\rightarrow VI}$** (one solvent molecule in the gas), **TS$_{ipC}^{ISIP\rightarrow VIII}$** (two solvent molecules in the gas), **TS$_7$** (one solvent molecule in the reaction field), and **TS$_9$** (two solvent molecules in the reaction field). Solvent reaction field optimized geometries as well as selected bond lengths during these processes are presented in Figure 5. Note that ISIPs **ipB^{ISIP}** and **ipC^{ISIP}**, or a couple of **ipB(s)^{ISIP}/ipC(s)^{ISIP}**, are stabilized by the two and three hydrogen bonds, respectively, between the oxygen atom of the isopropoxide anion and the N−H and O−H (one or two) of the propan-2-ol. Thus, the proton may be delivered to the isopropoxide anion by the media, rather than from the N−H of the cationic Ru complex. These questions will be addressed below.

Notably, even in the gas phase, the presence of one solvent molecule changed the one-step concerted mechanism to the stepwise mechanism discussed above. Thus, from the total six approaches examined, including one gas phase, one continuum solvent model, two discrete solvent models, and two mixed continuum/discrete solvent models, only the gas phase 1:1 reaction between **Ru-1** and acetone occurred via the three-bond asynchronous concerted pathway through a six-membered pericyclic transition state. Introduction separately of *nonspecific* or *specific* solvation of propan-2-ol or their combination into the DFT calculations suggests that a pericyclic mechanism[9d,12a] through a six-membered transition state is improbable in the liquid phase.

Upon introduction of explicit solvent molecules into the continuum solvent reaction field calculations, the H···Ru bond length in the ISIP increases from 1.88 Å in **ipA(s)^{ISIP}** via 1.92 Å

dx.doi.org/10.1021/ja3097674 | *J. Am. Chem. Soc.* 2013, 135, 2604−2619

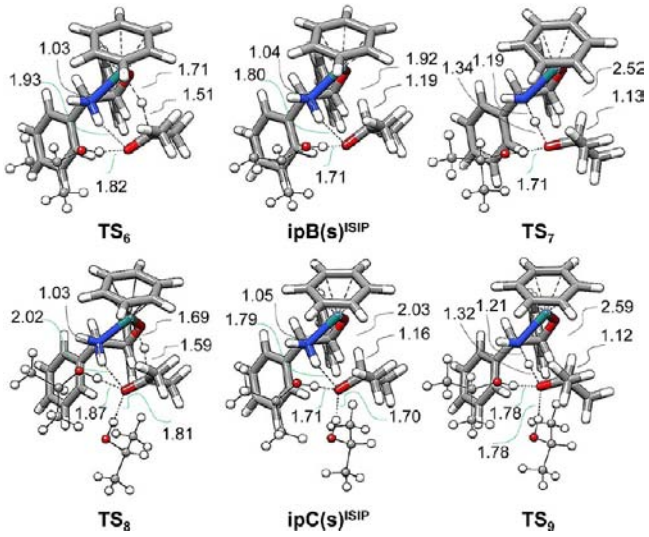

Figure 5. DFT/M06/SDD(Ru)/6-311++G**(C,H,N,O)/SMD-(propan-2-ol)-optimized geometries of the stationary points (minima or first-order saddle points) along the reaction coordinate between (*S*)-RuH[(*R*,*R*)-OCH(Ph)CH(Ph)NH_2](η^6-C_6H_6) (**Ru-1**) and acetone in the presence of one or two solvent molecules. Selected bond lengths are presented.

in **ipB(s)**^{ISIP} to 2.03 Å in **ipC(s)**^{ISIP}, and the C−H bond decreases from 1.21 Å in **ipA(s)**^{ISIP} via 1.19 Å in **ipB(s)**^{ISIP} to 1.16 Å in **ipC(s)**^{ISIP}, respectively (cf. 1.12 Å in "free" anion), as shown in Figure 5. Thus, the anion character as well as overall stability of the ISIP increases upon introduction of the solvent molecules. Note that a weak C−H···Ru hydrogen-bonding interaction is still present in all ISIPs; however, the C(H)···Ru distance increases from 3.06 Å in **ipA(s)**^{ISIP} via 3.08 Å in **ipB(s)**^{ISIP} to 3.15 Å in **ipC(s)**^{ISIP} upon introduction of solvent molecules. At the same time, both hydride and proton transfer barriers become lower in energy (Figure 4). The same is true for the gas phase. This tendency is expected, taking into account the cooperative effect in hydrogen bonding.[66] The endothermicity decreases in the order **1**→**ipA(s)**^{ISIP} < **5**→**ipB(s)**^{ISIP} < **7**→**ipC(s)**^{ISIP}, with the corresponding transition states becoming "earlier" in the character (see bond lengths during the hydride transfer in Figures 2 and 5), in agreement with Hammond's postulate.[67]

Similarly to the reaction between **1** and acetone in the reaction field described above, the barrier to the proton transfer within each ISIP was found to be slightly higher than that of the hydride transfer in the gas phase, as shown in Figure 4. In contrast, in the reaction field and notably for the transformation of **7**→**8** on the electronic energy scale, which is the most advanced among the models, the transition state corresponding to the hydride transfer is clearly rate-determining. The transition states shown in Figure 4, except $\mathbf{TS_7}$ and $\mathbf{TS_9}$, are the true transition states connecting 18e Ru hydrido complexes with 16e Ru amido complexes via ISIPs, as verified separately by the accurate IRC calculations.

On the other hand, IRC calculations from the transition structures $\mathbf{TS_7}$ (i1352 cm^{-1}) and $\mathbf{TS_9}$ (i1273 cm^{-1}) led to the identification of the outer-sphere ionic pair (OSIP)[62] intermediates **ipB(s)**^{OSIP} and **ipC(s)**^{OSIP}, respectively, as shown in Figure 6. The OSIPs are also stabilized by the ionic N−H···O^- hydrogen bond between the cation and the anion, however, the latter being placed in the second coordination

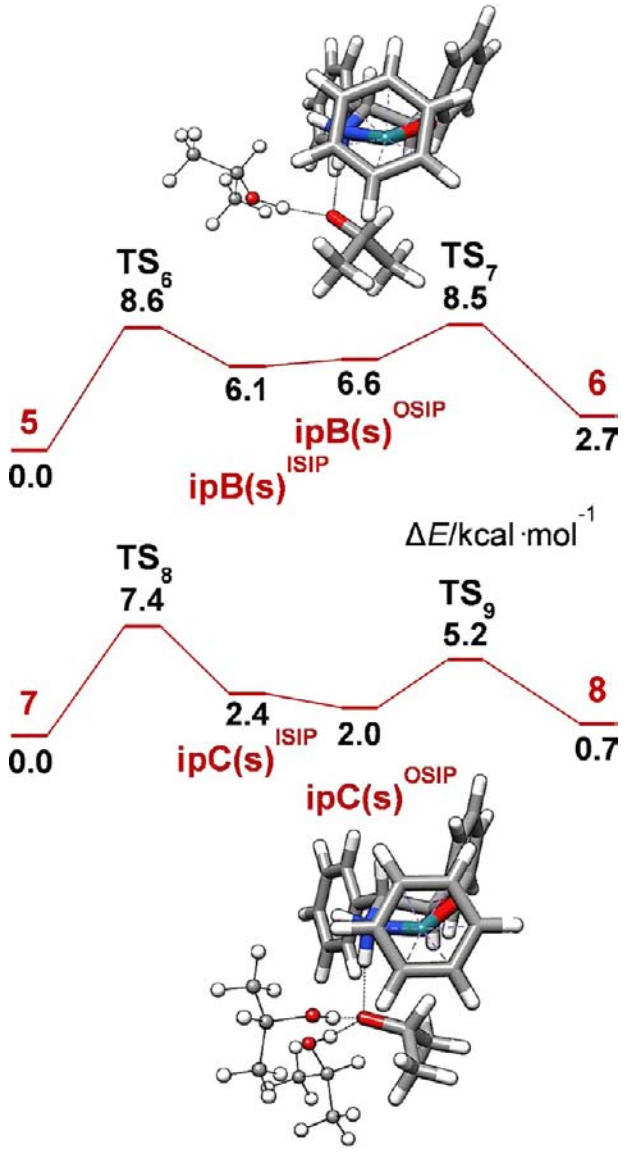

Figure 6. DFT/M06/SDD(Ru)/6-311++G**(C,H,N,O)/SMD-(propan-2-ol) energy profile of the reaction between **Ru-1** and acetone in the presence of one or two explicit solvent molecules. Intrinsic reaction coordinate for the transformations of **5**→**6** and **7**→**8**.

sphere. Because of this structural arrangement in the OSIP, the configuration around the ruthenium center is now almost square-planar, and there is significant loss of the weak, "non-classical" C−H···Ru hydrogen-bonding interaction (cf. the couple **ipA(s)**^{ISIP}/**ipA(s)**^{OSIP} described above). For example, in the stationary point located for the complex **ipC(s)**^{OSIP} in Figure 6, the distance $d_{C(H)\cdots Ru}$ is 3.53 Å and angle C−H···Ru is 141°, which can be compared with the significantly shorter distance $d_{C(H)\cdots Ru}$ of 3.15 Å and almost linear angle C−H···Ru of 161° in **ipC(s)**^{ISIP}. For **ipC(s)**^{OSIP} and **ipC(s)**^{ISIP}, the angle $CNT^{benzene}$−Ru−CNT^{NO} is 161° and 152°, respectively, whereas the RuNOC dihedral angle is 35° and 9°, correspondingly. The planarity of the dihedral angle RuNOC in the ISIP is crucial, because only under such an arrangement can the Ru−H/C−H be broken/formed, and the hydride transfer step can be viewed as corresponding to a one-bond[17a] concerted reaction. Thus, only one minimum with all six atoms lying practically in one plane exists for the ISIP. For the OSIP,

dx.doi.org/10.1021/ja3097674 | J. Am. Chem. Soc. 2013, 135, 2604−2619

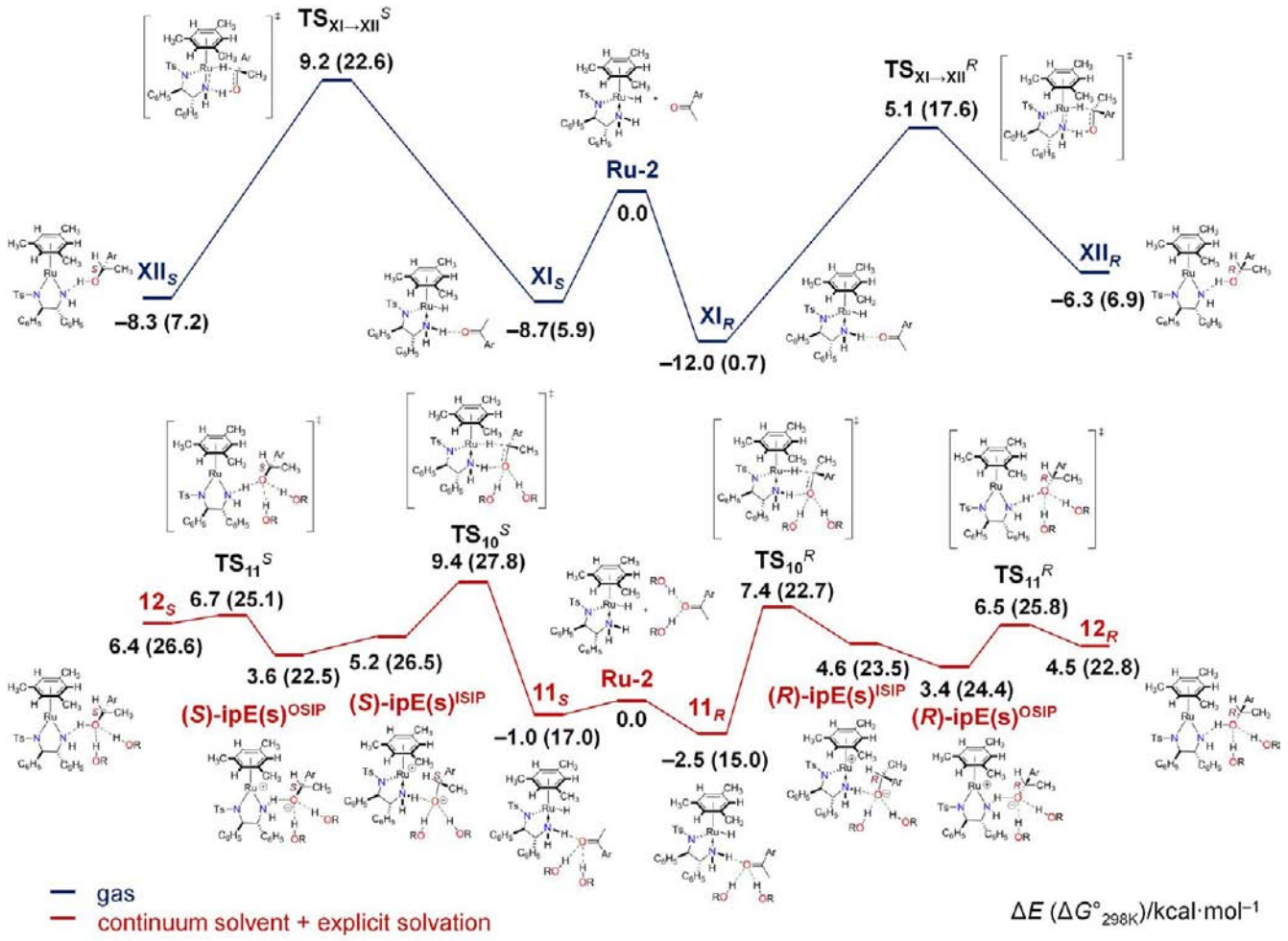

Figure 7. DFT/M06/SDD(Ru)/6-31G*(C,H,N,O,S) energy profile of the reaction between (*S*)-RuH[(*R,R*)-TsNCH(Ph)CH(Ph)NH$_2$](η^6-mesitylene) (**Ru-2**) and acetophenone to produce (*R*)-1-phenylethanol (*R*-pathway) and (*S*)-1-phenylethanol (*S*-pathway) in the gas phase or in the continuum solvent reaction field (SMD solvation model[39]) of propan-2-ol in the presence of two explicit solvent molecules. R = $CH(CH_3)_2$, Ar = C_6H_5.

in contrast, many different geometric isomers are possible, originating from rotation along the N−H···$^{-}$O−C bond as well as variation in the general position of the anion in the second coordination sphere,[68] each having a distinct activation barrier for the N−H proton transfer. Of note, the thermodynamic stability of the OSIP is reproduced only when at least two explicit solvent molecules are considered in the calculations. These two solvent molecules effectively stabilize the anion via two additional O−H···$^{-}$O−C hydrogen bonds. For example, **ipA(s)**^{OSIP} described above is 1.7 kcal/mol higher (ΔE) than **ipA(s)**^{ISIP} (reaction field), and **ipB(s)**^{OSIP} is only 0.5 kcal/mol higher (ΔE) than **ipB(s)**^{ISIP} (reaction field + one explicit solvent molecule), whereas **ipC(s)**^{OSIP} is already −0.4 kcal/mol lower (ΔE) than **ipC(s)**^{ISIP} (reaction field + two explicit solvent molecules). The same thinking is valid for the N−H proton transfer step, where the corresponding transition state is stabilized by H-bonding with solvent molecules. Thus, all further calculations were performed in the presence of two explicit solvent molecules.

Reaction of (*S*)-RuH[(*R,R*)-*p*-TsNCH(Ph)CH(Ph)NH$_2$](η^6-mesitylene) (Ru-2) with Acetone. The reaction between (*S*)-RuH[(*R,R*)-Tsdpen](η^6-mesitylene) (**Ru-2**) and acetone was also studied in the gas phase and in the solvent reaction field in the presence of two solvent molecules via the "solvated supermolecules" approach, allowing us to introduce *nonspecific* and *specific* solvation. This was done with the 6-31G* basis-set for the (C,H,N,O,S) atom block because of the high computational cost associated with the large molecules. Similar results were obtained in for reaction between **Ru-1** and acetone with the 6-311++G** and 6-31G* basis sets, although in the latter case all the relative energies are systematically ca. 1 kcal/mol higher in energy (see Figure S8). Similarly to **Ru-1**, a pericyclic three-bond asynchronous transition state was found in the gas phase, and a two-step profile was obtained in the solvent reaction field (see SI for details, Figure S11).

Reaction of (*S*)-RuH[(*R,R*)-*p*-TsNCH(Ph)CH(Ph)NH$_2$](η^6-mesitylene) (Ru-2) with Acetophenone. We next studied the reaction between (*S*)-RuH[(*R,R*)-Tsdpen](η^6-mesitylene) (**Ru-2**) and acetophenone to produce (*R*)- or (*S*)-1-phenylethanol. Chiral complex **Ru-2** catalyzes ATH of acetophenone (25 °C, 15 h, S/C = 200) from propan-2-ol to produce (*R*)-1-phenylethanol with 95% yield and 97% ee,[1a] corresponding to a 2.47 kcal/mol free energy difference[69] between the rate-determining diastereomeric transition states leading to different enantiomers. Proper computational analysis of the reaction between **Ru-2** and acetophenone producing (*R*)- or (*S*)-1-phenylethanol should include conformational and configurational searches. Such an analysis, however, is out of scope in

dx.doi.org/10.1021/ja3097674 | *J. Am. Chem. Soc.* 2013, 135, 2604−2619

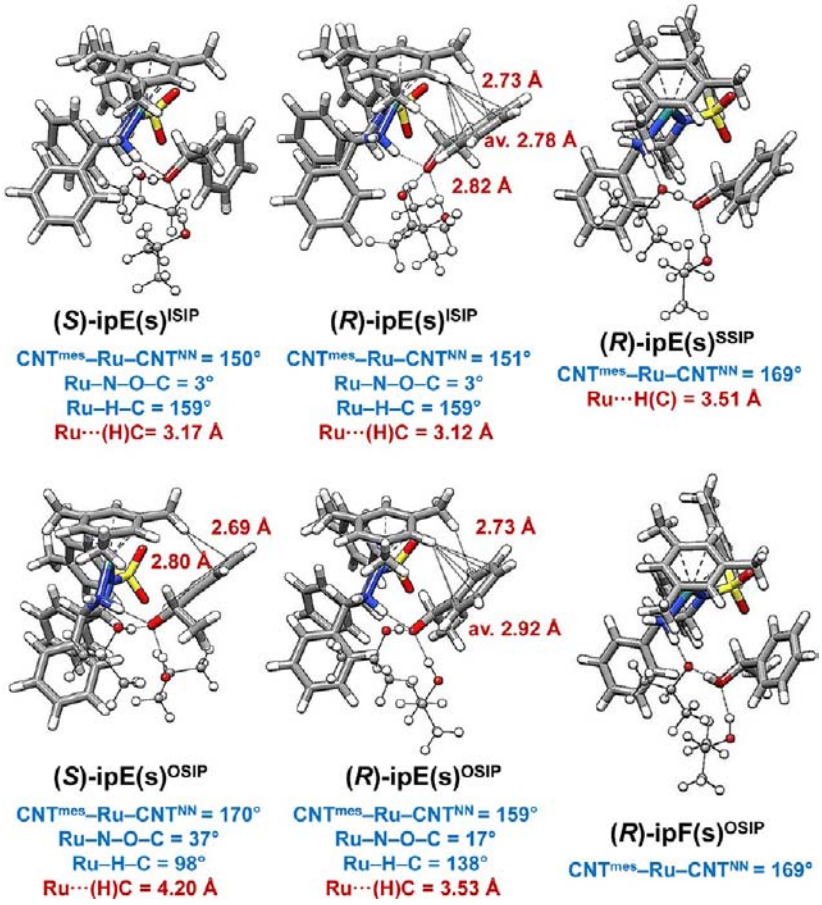

Figure 8. DFT/M06/SDD(Ru)/6-31G*(C,H,N,O,S)/SMD(propan-2-ol)-optimized geometries of the **ipE(s)**^{ISIP}, **ipE(s)**^{OSIP}, (*R*)-**ipE(s)**^{SSIP}, and (*R*)-**ipF(s)**^{OSIP} ion pairs. Selected structural parameters are presented.

this paper. Only a fixed configuration/conformation (R,R,R_N,S_{Ru},λ) of the complex **Ru-2** (see Chart S1) was considered in the reaction with acetophenone. This type of structural arrangement (R,R,R_N,S_{Ru},λ) was found for the similar 18e hydrido complex (*S*)-RuH[(*R*,*R*)-Tsdpen](η^6-*p*-cymene) in the solid state (X-ray structure).[10]

The 1:1 reaction of **Ru-2** and acetophenone to produce (*R*)-1-phenylethanol (*R*-pathway) and (*S*)-1-phenylethanol (*S*-pathway) in the gas phase proceeded through H-bonded adduct **XI** between the 18e Ru hydrido complex and acetophenone via the three-bond concerted asynchronous process through six-membred pericyclic transition structure $\mathbf{TS}_{XI\rightarrow XII}$ to produce H-bonded adduct **XII** between the 16 Ru amido complex and chiral 1-phenylethanol, as shown in Figure 7. The relative energy difference between the EDSs (transition states $\mathbf{TS}_{XI\rightarrow XII}{}^{R}$ vs $\mathbf{TS}_{XI\rightarrow XII}{}^{S}$) in the gas phase, 4.2 kcal/mol on the electronic energy scale and 5.0 kcal/mol on the free energy scale in favor of the *R*-enantiomer, is in qualitative agreement with the experimental value of 2.47 kcal/mol determined on the basis of the experimental 97% ee values.

In contrast, inclusion of nonspecific and specific solvation via the "solvated supermolecules" approach revealed the stepwise mechanism in which the activation barriers are significantly lowered relative to the gas phase, as shown in Figure 7. The transformations $\mathbf{11}_R\rightarrow\mathbf{12}_R$ and $\mathbf{11}_S\rightarrow\mathbf{12}_S$ to produce a hydrogen-bonded adduct between the 16e Ru-amido complex and (*R*)-1-phenylethanol and (*S*)-1-phenylethanol, respectively, proceed via the inner-sphere **ipE(s)**^{ISIP} and outer-sphere **ipE(s)**^{OSIP} contact ion-pair intermediates, correspondingly. The structural difference between **ipE(s)**^{ISIP} and **ipE(s)**^{OSIP} is the configuration around the ruthenium center and the position of the counteranion relative to the metal coordination sphere, being distorted octahedral with the anion in the first coordination sphere and square-planar with the anion in the second coordination sphere, as shown in Figure 8. The inner-sphere **ipE(s)**^{ISIP} is also stabilized by a weak "non-classical" C–H···Ru hydrogen-bonding interaction,[70] described above. This interaction preceeds the proton transfer to ruthenium,[71] being the reverse of the enantioselective hydride transfer, during which the hydrogen atom is repolarized.

Both **ipE(s)**^{ISIP} and **ipE(s)**^{OSIP} are stabilized by three hydrogen bonds, one N–H···O$^-$ with the ruthenium cation and two O–H···O$^-$ with two solvent molecules, respectively. For (*R*)-**ipE(s)**^{ISIP}, (*R*)-**ipE(s)**^{OSIP}, and (*S*)-**ipE(s)**^{OSIP}, however, additional stabilization via weak hydrogen bonding[64e,72] between C–H hydrogens of η^6-mesitylene ligand and the π-cloud of the phenylethanyl anion is present as shown in Figure 8. The N–H proton transfer could occur directly in **ipE(s)**^{ISIP} without any relegation of the anion to the second coordination sphere. However, similarly to the reaction of **Ru-2** or **Ru-1** with acetone described above, this pathway was found to be slightly energetically prohibitive (see [***i*681 cm**$^{-1}$]^{TS} and [***i*480 cm**$^{-1}$]^{TS} in Figure S12). A lower-energy N–H proton transfer pathway to the organic anion occurs effectively from the **ipE(s)**^{OSIP}, transition states $\mathbf{TS}_{11}{}^{R}$ (i1000 cm^{-1}) and $\mathbf{TS}_{11}{}^{S}$ (i1091 cm^{-1}) as shown in Figure 7.

dx.doi.org/10.1021/ja3097674 | *J. Am. Chem. Soc.* 2013, 135, 2604–2619

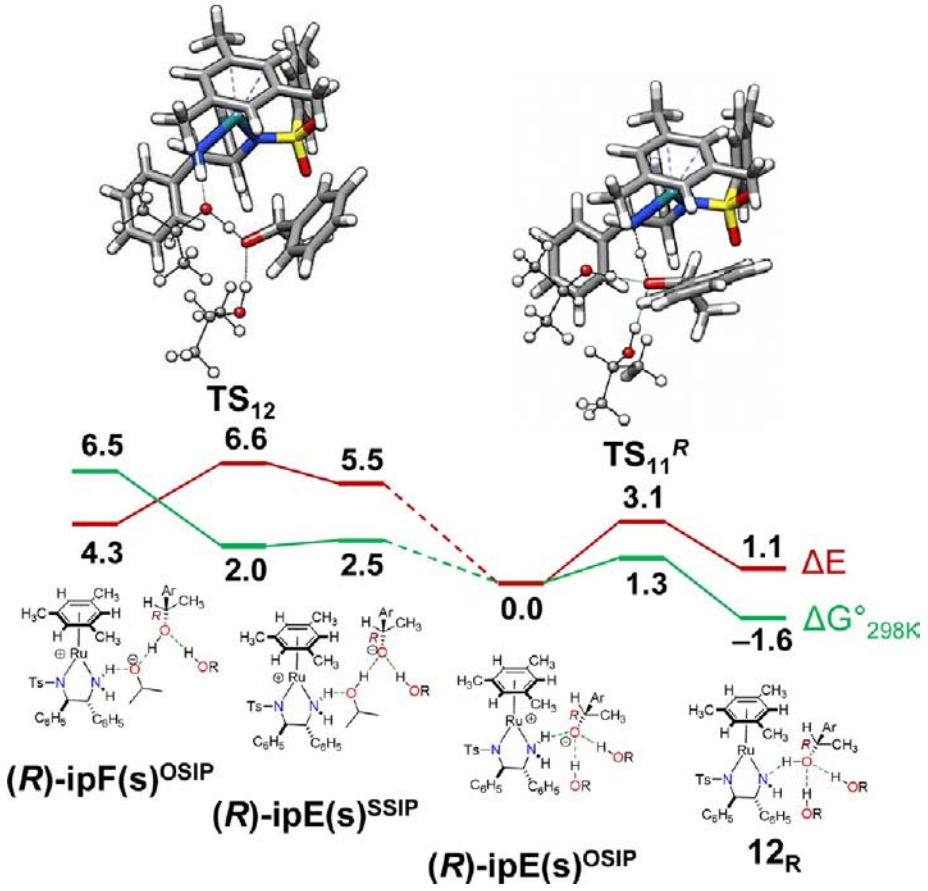

Figure 9. DFT/M06/SDD(Ru)/6-31G*(C,H,N,O,S)/SMD(propan-2-ol)-comparative energy profiles for proton transfer from the N−H bond of the Ru cation or the O−H proton of the propan-2-ol within the outer-sphere ion pair (*R*)-**ipE(s)**^{OSIP}. Energy in kcal/mol is calibrated relative to the (*R*)-**ipE(s)**^{OSIP}. R = $CH(CH_3)_2$, Ar = C_6H_5.

The *Re* face $\mathbf{11}_R$ and *Si* face $\mathbf{11}_S$ hydrogen-bonded adducts precede the EDS, which is the hydride transfer from the **Ru-2** to the C-atom of the acetophenone. Corresponding transition state $\mathbf{TS_{10}}^R$ (*i*433 cm^{-1}), leading to the *R*-enantiomer, is more stable than $\mathbf{TS_{10}}^S$ (*i*448 cm^{-1}), leading to *S*-enantiomer, by 2.0 kcal/mol on the electronic energy scale and 5.0 kcal/mol on the free energy scale. A similar energy profile was also obtained under the BLYP/C-PCM level of theory, where the corresponding energy difference between the EDSs is 2.2 kcal/mol on the electronic energy scale and 2.3 kcal/mol on the free energy scale, respectively (see Figure S12). Thus, both the M06 gas phase calculations and the M06/SMD or BLYP/C-PCM calculations with the inclusion of nonspecific and specific solvation effects correctly qualitatively predict the experimental enantioselectivity and sense of the enantioselection.[73]

To evaluate the possibility of proton transfer from the media, we have studied the O−H proton transfer from propan-2-ol to the oxygen atom of the (*R*)-1-phenylethoxide anion within the ion pair (*R*)-**ipE(s)**^{OSIP}. The latter could be also viewed as an (*R*)-1-phenylethoxide anion stabilized by three hydrogen bonds between the oxygen atom and the N−H hydrogen atom of the cationic Ru complex and two O−H protons of the propan-2-ol. A constrained PES scan performed along the O−H···O^- coordinate for one propan-2-ol molecule H-bonded to an (*R*)-1-phenylethoxide anion and subsequent transition state optimization revealed transition structure $\mathbf{TS_{12}}$ (*i*258 cm^{-1}), which corresponds to proton transfer along the O−H···O^- coordinate, as depicted in Figure 9. IRC calculations from this transition state revealed two minima, corresponding to ion pairs (*R*)-**ipE(s)**^{SSIP} and (*R*)-**ipF(s)**^{OSIP}, as shown in Figures 8 and 9. Complex (*R*)-**ipE(s)**^{SSIP} could be viewed as a solvent-shared ion pair,[62] obtained from (*R*)-**ipE(s)**^{OSIP} by involvement of one solvent molecule between the Ru cationic complex and the (*R*)-1-phenylethoxide anion.[74] The process (*R*)-**ipE(s)**^{OSIP}→(*R*)-**ipE(s)**^{SSIP} costs 2.5 kcal/mol on the free energy scale and is 1.2 kcal/mol higher than the energy of $\mathbf{TS_{11}}^R$, corresponding to proton transfer from the Ru complex to the (*R*)-1-phenylethoxide anion. Complex (*R*)-**ipF(s)**^{OSIP} could be viewed as an outer-sphere contact ion pair between the Ru cationic complex and the isopropoxide anion, which is additionally stabilized by one hydrogen bond with the (*R*)-1-phenylethanol.[75] Unfortunately, dissociation of the OSIP (*R*)-**ipE(s)**^{OSIP} into a solvent-shared ion pair, (*R*)-**ipE(s)**^{SSIP}, is only poorly modeled by the present calculations, since in reality each cation and anion is expected to be effectively solvated by a solvent shell, and thus more stabilized. As a result, the present calculations do not allow unambiguous discrimination among the possible mechanisms for the proton transfer, since more solvent molecules should be included in the cluster model.

Enantioselectivity. In the present work we have shown that the EDS of the catalytic cycle is the hydride transfer. The corresponding diastereomeric transition state is rate-determining.[47] The composition of the enantiomers (%ee) would be determined by the free energy difference between these two diastereomeric transition states leading to the opposite enantiomers. For the reaction between **Ru-1** and acetophenone

dx.doi.org/10.1021/ja3097674 | *J. Am. Chem. Soc.* 2013, 135, 2604−2619

in a continuum solvent reaction field, we have found for the S_{Ru} diastereomer that the weak C−H···π hydrogen bond[64e,72] between one C−H proton of the η^6-C_6H_6-ligand and the π-cloud of the approaching aromatic ketone, previously denoted as a CH/π attraction,[12b] is one of the stabilizing factors for the pathway leading to (*R*)-1-phenylethanol, as shown in Figure 10.

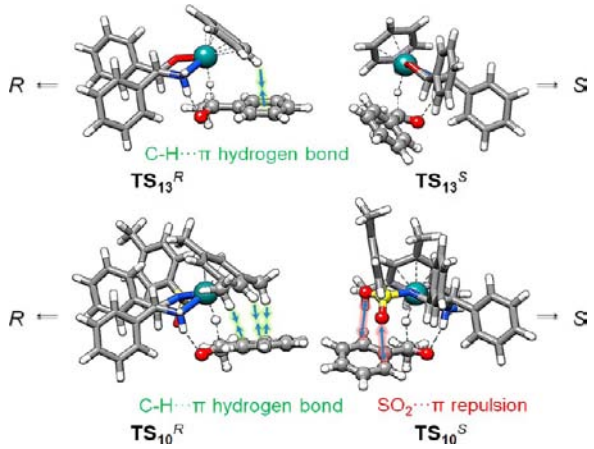

Figure 10. Identified stabilizing vs destabilizing factors of the transitions states leading to (*R*)- or (*S*)-1-phenylethanol. For **Ru-2**, explicit solvent molecules are omitted for clarity. The (R,R,S_{Ru},λ) structural arrangement is used. For **Ru-2**, the absolute configuration on the nitrogen NTs atom is *R*.

The transition state of the hydride transfer, $\mathbf{TS_{13}}^R$ (i324 cm^{-1}) is 0.35 kcal/mol more stable on the free energy scale but −1.10 kcal/mol less stable on the electronic energy scale than $\mathbf{TS_{13}}^S$ (i367 cm^{-1}), leading to the opposite enantiomer. This is comparable with the value of 0.02 kcal/mol, determined[69] from the experimentally obtained ee value of 2%, where the major product is (*R*)-1-phenylethanol.[2] Examination of $\mathbf{TS_{13}}^R$ reveals that a hydrogen atom is directed to the center[76] of the acetophenone aromatic ring with a distance of 2.69 Å and angle C−H−CNT^{arene} of 142°, where CNT^{arene} is a centroid of the acetophenone aromatic ring. The corresponding C−H bond length, however, is only slightly elongated by 0.001 Å relative to other C−H bonds of the η^6-C_6H_6 ligand (Figure 10). The Mulliken charge on this hydrogen atom, q_H = 0.055, is decreased relative to an averaged charge of unbound hydrogen atoms, q_H = 0.237.[77]

For the reaction between **Ru-2** and acetophenone, three weak hydrogen bonds between one C(sp^2)−H proton and two C(sp^3)−H protons of the η^6-mesitylene ligand, correspondingly, and the π-cloud of the approaching acetophenone were identified as stabilizing factors for the pathway leading to the major enantiomer, (*R*)-1-phenylethanol, transition structure $\mathbf{TS_{10}}^R$ in Figure 10. The distance between the proton and the center of the acetophenone aromatic ring is 2.78 Å. This C(sp^2)−H proton is directed directly to the center of the acetophenone aromatic ring, whereas two other C(sp^3)−H protons are directed only to the nearest carbon atoms, with distances of 2.65 and 2.86 Å, respectively. The corresponding

Scheme 2. Revised Catalytic Cycle(s) of the Asymmetric Transfer Hydrogenation Catalyzed by RuH[(*R*,*R*)-XCH(Ph)CH(Ph)NH_2](η^6-arene): Formation of the Major Enantiomer Is Shown

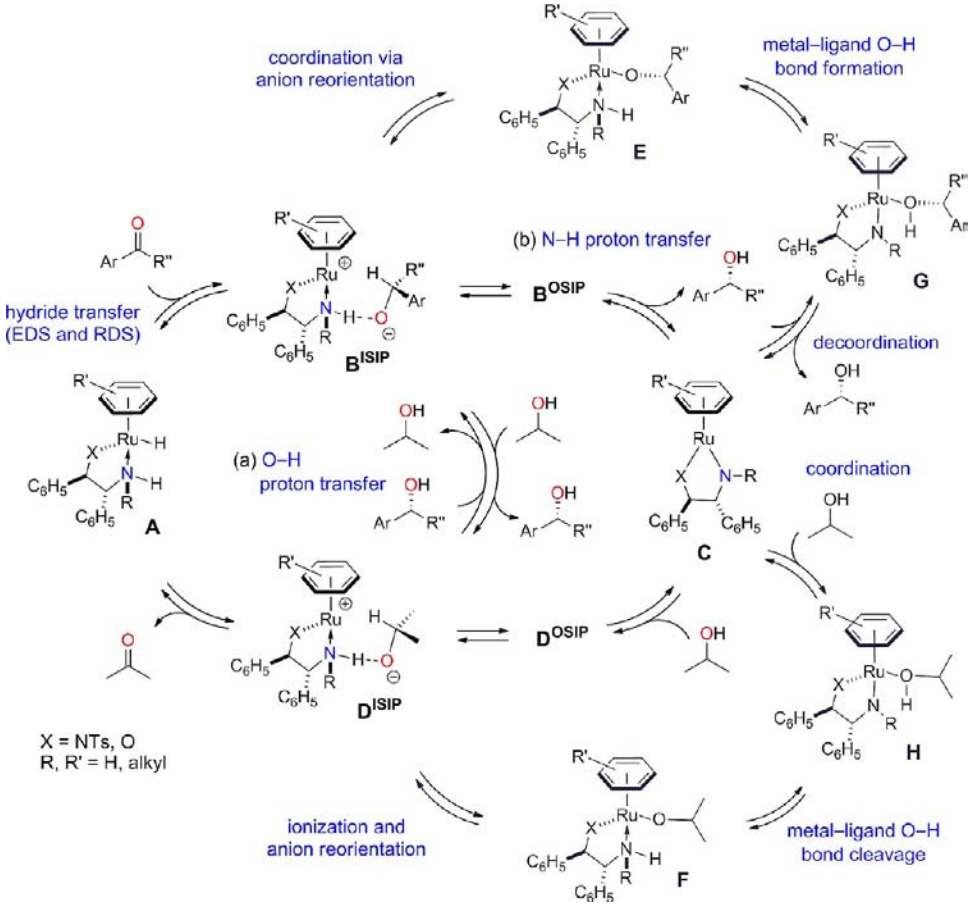

dx.doi.org/10.1021/ja3097674 | J. Am. Chem. Soc. 2013, 135, 2604−2619

Mulliken charges are also found to be decreased by Δq_H = −0.015 and −0.018 for C(sp^2)−H and C(sp^3)−H protons, respectively. The angle C(sp^2)−H−CNT^{arene} is 143°. In contrast, the transition state leading to the minor enantiomer, (*S*)-1-phenylethanol, is destabilized by the repulsion between the SO_2 group oxygen atoms of the Ts moiety and the π-cloud of the approaching aromatic ketone, transition structure $\mathbf{TS_{10}}^S$ in Figure 10. The distances between the two oxygen atoms and the closest carbon atoms in acetophenone, 3.40 and 3.49 Å, respectively, are comparable with the sum of the corresponding van der Waals radii (3.50 Å). Thus, in the case of **Ru-2**, both stabilization from three C−H···π hydrogen bonds and destabilization from SO_2/π repulsion originating from the NTs group cooperate to increase the free energy difference between the diastereomeric transition states, leading to different enantiomers and contributing, among other factors, to the excellent ee value (97%).

The presence of a NSO_2R group on the DPEN ligand is the strict reason why the Ru^{II}(η^6-arene) complexes bearing *N*-sulfonylated DPEN give better ee's (90−99% ee) than corresponding Ru^{II}(η^6-arene) complexes bearing chiral 2-amino alcohol auxiliaries (2−92% ee). For example, complex (*S*)-RuH[(*R*,*R*)-*p*-TsNCH(Ph)CH(Ph)NH_2](η^6-C_6H_6), which differs from **Ru-1** only by replacement of the O atom in the amino alcohol ligand with NTs, catalyzes the ATH of acetophenone, giving the final chiral product with 90% ee[1a] (cf. 2% for **Ru-1**). Thus, the crucial factor for achieving high enantioselectivity for this complex is actually destabilization of the diastereomeric transition structure, leading to the minor enantiomer via SO_2/π repulsion.

Catalytic Cycle. Based on the present work and overall experimental and theoretical data accumulated so far, the mechanism of the ATH catalyzed by bifunctional ruthenium complexes could follow two catalytic cycles, (a) and (b) in Scheme 2. In both cases, the first step is the enantio-determining hydride transfer from the neutral amine hydrido complex **A** through the hydrogen-bonded intermediate **A**···O=CRR′ (NH···O=C), leading to the inner-sphere[62] ion pair $\mathbf{B}^{ISIP}$ stabilized primarily by an ionic hydrogen bond between the cation and the anion (NH···$^-$O−C), as shown in Scheme 2. The transition state corresponding to the hydride transfer is also rate-determining.[47] The inner-sphere contact ion pair $\mathbf{B}^{ISIP}$ could be involved in at least four equilibria.

The first equilibrium involves relegation of the organic anion to the second coordination sphere of the metal-containing moiety to afford the more stable outer-sphere[62] ion pair $\mathbf{B}^{OSIP}$, which is also stabilized by an ionic hydrogen bond via the NH···$^-$O−C fragment. The structural difference between $\mathbf{B}^{ISIP}$ and $\mathbf{B}^{OSIP}$ is the configuration around the ruthenium atom, being distorted octahedral in the first case and square-planar in the second. We also noted the importance of the planarity of the dihedral angle RuNOC as well as the presence of a "non-classical" C−H···Ru hydrogen-bonding interaction[64] in $\mathbf{B}^{ISIP}$. Only under such an arrangement can C−H/Ru−H be broken/formed, and the hydride transfer step can be viewed as corresponding to a one-bond[17a] concerted reaction. The C−H···Ru hydrogen bond preceeds the proton transfer to ruthenium from the organic anion,[71] being the reverse reaction of the enantioselective hydride transfer. Thus, only one minimum, corresponding to $\mathbf{B}^{ISIP}$, is possible, similarly to the "lock and key" model in enzymatic reactions.[78] Only under such an arrangement is the enantioselectivity of the reaction determined via the free energy difference of the rate-determining diastereomeric transition states. For $\mathbf{B}^{OSIP}$, in contrast, different isomers originating from rotation along the NH···$^-$O−C bond as well as in general the position of the anion in the second coordination sphere are possible.

The second equilibrium is the formation of the ion pair **D** (or a couple of $\mathbf{D}^{ISIP}/\mathbf{D}^{OSIP}$) by reaction with the solvent molecule. During this step the product is released, and thus the proton source for the ketone is the protic solvent. The ion pair **D** regenerates **A** via acetone releasing, and this would close the first catalytic cycle. Note that in this cycle the 16e amido complex **C** is not the reaction intermediate.

The third equilibrium is the reversible N−H proton transfer to afford amido complex **C**. This transfer occurs effectively only in $\mathbf{B}^{OSIP}$, because according to calculations the proton transfer in the six-membered quasicycle within $\mathbf{B}^{ISIP}$ is energetically prohibitive. During this step the final product is released, and thus the proton source for the ketone is the amine group of the cation of the Ru complex **B**. **C** regenerates **A** via reaction with propan-2-ol and through ion pair intermediate **D**, and this would close the second catalytic cycle.

The fourth equilibrium in which $\mathbf{B}^{ISIP}$ is involved is reversible O-coordination of the anion on the metal via its reorientation to afford (*R*)-1-phenylethoxo complex **E**. This process occurs via a single transition state. Complex **E** is an off-loop species; i.e., it exists in thermal equilibrium during the catalytic reaction at lower energy than the rate-determining barrier but is not directly involved in the minimum energy pathway of the catalytic cycle. **E** can be also obtained from **C** through Werner-type complex **G** and the following O−H bond cleavage based on metal−ligand cooperation, i.e., without change in the formal oxidation state of the metal. Similarly, the isopropyloxo complex **F** can be obtained directly from $\mathbf{D}^{ISIP}$ via anion reorientation or through Werner-type intermediate complex **H**. Similarly to (*R*)-1-phenylethoxo complex **E**, isopropyloxo complex **F** is an off-loop species. One of these compounds can reasonably be a resting state for the catalyst.

Calculations performed for complex **Ru-1** and acetone (*vide supra*) suggest that, for RuH[(*R*,*R*)-OCH(Ph)CH(Ph)NH_2](η^6-arene) complexes, the corresponding isopropyloxo complex of type **F**, as shown in Scheme 2, is obtained via slightly more favorable coordination of alcohol on the 16e amido complex **C** to produce **H** and the following O−H bond cleavage based on metal−ligand cooperation. The transition state associated with direct anion reorientation in the corresponding $\mathbf{D}^{ISIP}$ ($\mathbf{TS_3}$ in Figure 3) to afford **F** was found to be slightly higher in energy (*vide supra*). At this point, comparison with available experimental data can be done. Complexes RuH[(*R*,*R*)-OCH(Ph)CH(Ph)NH_2](η^6-arene) are typically considered to be analogues of RuH[(*R*,*R*)-*p*-TsNCH(Ph)CH(Ph)NH_2](η^6-arene) that are hardly isolable.[2] Complex (*R*)-RuH[(*S*,*S*)-*p*-TsNCH(Ph)CH(Ph)NH_2](η^6-*p*-cymene) reacts with acetone in toluene to afford the 16e violet amido complex Ru[(*S*,*S*)-*p*-TsNCH(Ph)CH(Ph)NH](η^6-*p*-cymene) and propan-2-ol as kinetic reaction products.[10] In contrast, the related Noyori hydrogenation catalyst Ru(H)$_2$(diamine)(diphosphine) gives the alkoxo complex Ru(H)(OR)(diamine)(diphosphine) as a kinetic product in THF.[26] Both compounds are similar in that they have the same bifunctional HRuNH moiety. The only way to explain the formation of Ru(H)(OR)(diamine)-(diphosphine) is to assume the ISIP intermediate on the reaction coordinate that would provide the alkoxo complex via lower energy anion reorientation, rather than N−H proton transfer. This proposition has been recently confirmed

dx.doi.org/10.1021/ja3097674 | J. Am. Chem. Soc. 2013, 135, 2604−2619

computationally by using DFT/M06 with the polarizable continuum model (PCM) in propan-2-ol. Simplified model $Ru(H)_2$(diamine)(diphosphine) was reported[79] to react with acetophenone via an ion-pair intermediate similar to the ISIPs described here, which then gives the alkoxo product via a lower energy anion reorientation.

Thus, the intermediate formation of ion pairs allows rationalization of all known experimental data. Since the ion pair is less populated (higher in energy) than the corresponding hydrido and amido complexes, it probably could not be detected in the stoichiometric experiments by classical spectroscopy techniques, including slow methods such as NMR. Formation of a metastable ion pair intermediate is in agreement with the original Noyori–Ikariya NMR-based kinetic studies, where the interconversion between the 16e amido and the 18e hydrido Ru complexes by the action of an alcohol or ketone was proposed as an alternatively to the concerted three-bond reaction, to take place via a *short-lived intermediate*.[10] The ion pair intermediate in the related transfer hydrogenation catalyzed by bifunctional electron-richer Rh[80] and Ir[81] was found recently in the gas phase calculations and in one case in the continuum solvent reaction field for Os.[82]

The catalytic cycle in Scheme 2, similar to the one presented in Scheme 1, follows the out-of-sphere nonclassical pathway of the hydride transfer. The role of the metal in these transformations is to transfer the hydride, whereas the role of the ligand's N–H is to "fix" the approaching ketone via important hydrogen bond formation. The present work does not allow unambiguous discrimination between catalytic cycles (a) and (b), which differ only by the second proton transfer step. Both cycles, depending on the exact conditions, could operate; however, cycle (a) seems to be more probable, especially with increasing solvent polarity. Meijer and co-workers had come to similar conclusions in their *ab initio* molecular dynamics study,[30,31] although the discrete solvation model did not identify several intermediates.

The catalytic cycle presented in Scheme 2 and the overall mechanism based on the less-populated ISIP intermediate could be applied to rationalize the observed acceleration in reaction rates in more polar media reported by Xiao and Liu[20] and others.[24,83] Since the rate-determining hydride transfer step has ionic nature, rather than a neutral pericycle, the reaction barrier is expected to decrease in more polar media.[48a] In general, the "ionic cycle" is expected to be strongly sensitive to the media polarity as well as to the ionic strength of the media, which can be affected by the additives, including alkoxide salts. It was shown that media modification could change the sense of the enantioface selection in the ATH with the example of several polycyclic *meso*-compounds catalyzed by Noyori–Ikariya catalyst RuH[(*R*,*R*)-Tsdpen](η^6-arene).[33] Notably, the ion pair mechanism can also essentially explain the solvent-based reversal of the sense of enantioinduction, which can be rationalized in terms of "homo-/heterosolvation" of the ions, when cation and anion are solvated preferentially by different solvents.[84]

CONCLUSIONS

We have evaluated the reactions between unabridged chiral models of the ruthenium hydride complexes (*S*)-RuH[(*R*,*R*)-OCH(Ph)CH(Ph)NH_2](η^6-benzene) (**Ru-1**) and (*S*)-RuH-[(*R*,*R*)-Tsdpen](η^6-mesitylene) (**Ru-2**) with acetone or acetophenone in the framework of the density functional theory by using continuum, discrete, and mixed continuum/discrete solvation models via a "solvated supermolecules" approach. By including *specific* or/and *nonspecific* solvation effects, we have shown that propan-2-ol contributes to the asynchronicity of the reaction to such an extent that the mechanism changes from a three-bond asynchronous concerted reaction in the gas phase to a two-step process in solution, involving a higher energy contact ion pair intermediate. The two steps are (i) enantio-determining hydride transfer (also RDS) and (ii) proton transfer. The calculations suggest that the proton source for the produced chiral RO^- anion may be either the amine group of the cationic Ru complex or, more likely, a protic solvent molecule. In the latter case, the reaction may not necessarily proceed via the 16e amido complex Ru[(*R*,*R*)-XCH(Ph)CH(Ph)NH](η^6-arene). The origin of the enantio-selectivity is discussed in terms of the newly formulated mechanism.

ASSOCIATED CONTENT

Supporting Information

Cartesian coordinates for all optimized compounds, tables of energy data, complete ref 37, and other details. This material is available free of charge via the Internet at http://pubs.acs.org.

AUTHOR INFORMATION

Corresponding Author

tikariya@apc.titech.ac.jp

Notes

The authors declare no competing financial interest.

ACKNOWLEDGMENTS

We thank the MEXT for the Grant-in-Aid for Scientific Research (S) (No. 22225004), the G-COE Program, Grant-in-Aid for Scientific Research for JSPS Postdoctoral Fellows (10F00344). PAD thanks the JSPS for the Postdoctoral Research fellowship. We thank also Prof. DSc. Ilya D. Gridnev (Tohoku University, Sendai) for useful discussions and comments.

REFERENCES

(1) (a) Hashiguchi, S.; Fujii, A.; Takehara, J.; Ikariya, T.; Noyori, R. *J. Am. Chem. Soc.* **1995**, *117*, 7562. (b) Fujii, A.; Hashiguchi, S.; Uematsu, N.; Ikariya, T.; Noyori, R. *J. Am. Chem. Soc.* **1996**, *118*, 2521. (c) Uematsu, N.; Fujii, A.; Hashiguchi, S.; Ikariya, T.; Noyori, R. *J. Am. Chem. Soc.* **1996**, *118*, 4916.

(2) Takehara, J.; Hashiguchi, S.; Fujii, A.; Inoue, S.-i.; Ikariya, T.; Noyori, R. *Chem. Commun.* **1996**, 233.

(3) *Topics in Organometallic Chemistry: Bifunctional Molecular Catalysis*; Eds. Ikariya, T.; Shibasaki, M., Springer, 2011; Vol. 37.

(4) Ikariya, T.; Blacker, A. J. *Acc. Chem. Res.* **2007**, *40*, 1300.

(5) According to the Woodward–Hoffmann definition, "reactions in which all first-order changes in bonding relationship take place in concert on a closed curve" See ref 6 or: Woodward, R. B.; Hoffmann, R. *The Conservation of Orbital Symmetry*; Verlag Chemie, GmbH: Weinheim, 1970.

(6) Woodward, R. B.; Hoffmann, R. *Angew. Chem., Int. Ed. Engl.* **1969**, *8*, 781.

(7) The term "transition state" is consistently misapplied. It describes only the set of states or energy levels at the saddle point along the minimum energy reaction path. This point was suggested to be called a "transition structure". For discussions, see ref 8 and ref 48a, p 147. In this work we use both terms synonymously.

(8) (a) Laidler, K. J. *J. Chem. Educ.* **1988**, *65*, 540. (b) Bauer, S. H.; Wilcox, C. F. *J. Chem. Educ.* **1995**, *72*, 13. (c) Houk, K. N.; Li, Y.; Evanseck, J. D. *Angew. Chem., Int. Ed.* **1992**, *31*, 682. (d) Hoffmann, R.; Tantillo, D. J. *Angew. Chem., Int. Ed.* **2003**, *42*, 5877. (e) Lewars, E. G.

Computational Chemistry: Introduction to the Theory and Applications of Molecular and Quantum Mechanics, 2nd ed.; Springer: Berlin, 2011.
(9) (a) Ikariya, T. *Bull. Chem. Soc. Jpn.* **2011**, *84*, 1. (b) Ikariya, T.; Murata, K.; Noyori, R. *Org. Biomol. Chem.* **2006**, *4*, 393. (c) Samec, J. S. M.; Bäckvall, J.-E.; Andersson, P. G.; Brandt, P. *Chem. Soc. Rev.* **2006**, *35*, 237. (d) Noyori, R.; Yamakawa, M.; Hashiguchi, S. *J. Org. Chem.* **2001**, *66*, 7931. (e) Noyori, R.; Hashiguchi, S. *Acc. Chem. Res.* **1997**, *30*, 97.
(10) Haack, K.-J.; Hashiguchi, S.; Fujii, A.; Ikariya, T.; Noyori, R. *Angew. Chem., Int. Ed.* **1997**, *36*, 285.
(11) Casey, C. P.; Johnson, J. B. *J. Org. Chem.* **2003**, *68*, 1998.
(12) (a) Yamakawa, M.; Ito, H.; Noyori, R. *J. Am. Chem. Soc.* **2000**, *122*, 1466. (b) Yamakawa, M.; Yamada, I.; Noyori, R. *Angew. Chem., Int. Ed.* **2001**, *40*, 2818.
(13) Alonso, D. A.; Brandt, P.; Nordin, S. J. M.; Andersson, P. G. *J. Am. Chem. Soc.* **1999**, *121*, 9580.
(14) Petra, D. G. I.; Reek, J. N. H.; Handgraaf, J.-W.; Meijer, E. J.; Dierkes, P.; Kamer, P. C. J.; Brussee, J.; Schoemaker, H. E.; Van, L. P. W. N. M. *Chem.—Eur. J.* **2000**, *6*, 2818.
(15) Handgraaf, J. W.; Reek, J. N. H.; Meijer, E. J. *Organometallics* **2003**, *22*, 3150.
(16) Václavík, J. i.; Kuzma, M.; Přech, J.; Kačer, P. *Organometallics* **2011**, *30*, 4822.
(17) (a) Dewar, M. J. S. *J. Am. Chem. Soc.* **1984**, *106*, 209. (b) Borden, W. T.; Loncharich, R. J.; Houk, K. N. *Annu. Rev. Phys. Chem.* **1988**, *39*, 213. (c) Strauss, C. E. M.; Houston, P. L. *J. Phys. Chem.* **1990**, *94*, 8751.
(18) Marvet, U.; Dantus, M. *Chem. Phys. Lett.* **1996**, *256*, 57.
(19) (a) Kim, S. K.; Pedersen, S.; Zewail, A. H. *J. Chem. Phys.* **1995**, *103*, 477. (b) Pedersen, S.; Herek, J. L.; Zewail, A. H. *Science* **1994**, *266*, 1359.
(20) Wu, X.; Liu, J.; Di, T. D.; Iggo, J. A.; Catlow, C. R. A.; Bacsa, J.; Xiao, J. *Chem.—Eur. J.* **2008**, *14*, 7699.
(21) Bell, R. P. *Chem. Soc. Rev.* **1974**, *3*, 513.
(22) In their work, however, only the energetics was taken into account; i.e., the energies were calculated on the gas phase optimized geometries (single point) using the polarized continuum model (PCM), rather than optimizing the geometries directly in the solvent reaction field.
(23) (a) Reichardt, C. *Pure Appl. Chem.* **1982**, *54*, 1867. (b) Kosower, E. M. *Introduction to Physical Organic Chemistry*; Wiley: New York, 1968.
(24) Tanis, S. P.; Evans, B. R.; Nieman, J. A.; Parker, T. T.; Taylor, W. D.; Heasley, S. E.; Herrinton, P. M.; Perrault, W. R.; Hohler, R. A.; Dolak, L. A.; Hester, M. R.; Seest, E. P. *Tetrahedron: Asymmetry* **2006**, *17*, 2154.
(25) Sandoval, C. A.; Ohkuma, T.; Muniz, K.; Noyori, R. *J. Am. Chem. Soc.* **2003**, *125*, 13490.
(26) (a) Takebayashi, S.; Dabral, N.; Miskolzie, M.; Bergens, S. H. *J. Am. Chem. Soc.* **2011**, *133*, 9666. (b) Takebayashi, S.; Bergens, S. H. *Organometallics* **2009**, *28*, 2349. (c) Hamilton, R. J.; Bergens, S. H. *J. Am. Chem. Soc.* **2008**, *130*, 11979.
(27) Koike, T.; Ikariya, T. *Organometallics* **2005**, *24*, 724.
(28) Moasser, B. *Aqueous Metal-Ligand Bifunctional Hydrogenation of Carbon Dioxide*; 48059-G3; 55th Annual Report on Research 2010 Under Sponsorship of the ACS Petroleum Research Fund, 2010.
(29) Koike, T.; Ikariya, T. *Adv. Synth. Catal.* **2004**, *346*, 37.
(30) Handgraaf, J.-W.; Meijer, E. J. *J. Am. Chem. Soc.* **2007**, *129*, 3099.
(31) Pavlova, A.; Meijer, E. J. *ChemPhysChem* **2012**, *13*, 3492.
(32) In their first paper, however, a synchronous concerted reaction via a six-membered pericyclic transition state was proposed. See ref 12a.
(33) Clay, D. R.; McIntosh, M. C. *Tetrahedron Lett.* **2012**, *53*, 1691.
(34) (a) Carmona, D.; Lahoz, F. J.; Garcia-Orduna, P.; Oro, L. A.; Lamata, M. P.; Viguri, F. *Organometallics* **2012**, *31*, 3333. (b) Elliott, A. G.; Green, A. G.; Diaconescu, P. L. *Dalton Trans.* **2012**, *41*, 7852. (c) Hong, Y.; Tan, H.; Qiu, J.; Shen, L. *Synth. React. Inorg., Met.-Org., Nano-Met. Chem.* **2012**, *42*, 502. (d) Ibn, E. A. M. S.; El, A. M. A.; Dahdouh, A.; Roussel, P.; Suisse, I.; Mortreux, A. *Chirality* **2012**, *24*, 675. (e) Landwehr, A.; Dudle, B.; Fox, T.; Blacque, O.; Berke, H. *Chem.—Eur. J.* **2012**, *18*, 5701. (f) Nordin, M.; Liao, R.-Z.; Ahlford, K.; Adolfsson, H.; Himo, F. *ChemCatChem* **2012**, *4*, 1095. (g) O, W. W. N.; Lough, A. J.; Morris, R. H. *Organometallics* **2012**, *31*, 2152. (h) Zhou, X.; Wu, X.; Yang, B.; Xiao, J. *J. Mol. Catal. A: Chem.* **2012**, *357*, 133. (i) Madrigal, D.; Cooksy, A. L.; Somanathan, R. *Comp. Theor. Chem.* **2012**, *999*, 105. (j) Štefane, B.; Požgan, F. In *Hydrogenation*; Karamé, I., Ed.; InTech: 2012; p 31.
(35) It was important to use the real catalysts in the computations, since it is known that even slight simplification of the catalyst structure can result in a significant loss of the activity and enantioface selectivity.
(36) (a) Kohn, W.; Sham, L. J. *Phys. Rev.* **1965**, *140*, A1133. (b) Hohenberg, P.; Kohn, W. *Phys. Rev.* **1964**, *136*, B864.
(37) Frisch, M. J.; et al. *Gaussian 09*, revision C.01; Gaussian, Inc.: Wallingford, CT, 2009.
(38) http://www.gsic.titech.ac.jp/en
(39) Marenich, A. V.; Cramer, C. J.; Truhlar, D. G. *J. Phys. Chem. B* **2009**, *113*, 6378.
(40) (a) Zhao, Y.; Truhlar, D. G. *Acc. Chem. Res.* **2008**, *41*, 157. (b) Zhao, Y.; Truhlar, D. *Theor. Chim. Acta* **2008**, *120*, 215.
(41) Becke, A. D. *Phys. Rev. A* **1988**, *38*, 3098.
(42) (a) Cossi, M.; Rega, N.; Scalmani, G.; Barone, V. *J. Comput. Chem.* **2003**, *24*, 669. (b) Barone, V.; Cossi, M. *J. Phys. Chem. A* **1998**, *102*, 1995.
(43) Fukui, K. *Acc. Chem. Res.* **1981**, *14*, 363.
(44) Pettersen, E. F.; Goddard, T. D.; Huang, C. C.; Couch, G. S.; Greenblatt, D. M.; Meng, E. C.; Ferrin, T. E. *J. Comput. Chem.* **2004**, *25*, 1605.
(45) (a) Carlsson, J.; Aqvist, J. *J. Phys. Chem. B* **2005**, *109*, 6448. (b) Chang, C. E.; Chen, W.; Gilson, M. K. *J. Chem. Theor. Comput.* **2005**, *1*, 1017. (c) Singh, N.; Warshel, A. *J. Phys. Chem. B* **2009**, *113*, 7372.
(46) (a) Dub, P. A.; Poli, R. *J. Mol. Catal. A* **2010**, *324*, 89. (b) Kozuch, S.; Lee, S. E.; Shaik, S. *Organometallics* **2009**, *28*, 1303. (c) Braga, A. A. C.; Ujaque, G.; Maseras, F. *Organometallics* **2006**, *25*, 3647. (d) Ardura, D.; López, R.; Sordo, T. L. *J. Phys. Chem. B* **2005**, *109*, 23618. (e) Leung, B. O.; Reid, D. L.; Armstrong, D. A.; Rauk, A. *J. Phys. Chem. A* **2004**, *108*, 2720. (f) Cooper, J.; Ziegler, T. *Inorg. Chem.* **2002**, *41*, 6614.
(47) Kozuch, S.; Shaik, S. *Acc. Chem. Res.* **2010**, *44*, 101.
(48) (a) Reichardt, C.; Welton, T. *Solvents and Solvent Effects in Organic Chemistry*; 4th ed.; Wiley-VCH, 2010; (b) Karelson, M. M.; Katritzky, A. R.; Zerner, M. C. *Int. J. Quantum Chem.* **1986**, *30*, 521.
(49) (a) Feig, M. *Modeling Solvent Environments: Applications to Simulations of Biomolecules*; Wiley: Chichester, 2010. (b) Jensen, L.; van Duijnen, P. T.; Snijders, J. G. *J. Chem. Phys.* **2003**, *118*, 514. (c) Tomasi, J.; Mennucci, B.; Cappelli, C. In *Handbook of Solvents*; Wypych, G., Ed.; ChemTec Publishing: Toronto and William Andrew Publishing: New York, 2001. (d) Tomasi, J.; Persico, M. *Chem. Rev.* **1994**, *94*, 2027. (e) Tapia, O.; Bertrán, J. *Solvent Effects and Chemical Reactivity*; Springer: Berlin, 1996.
(50) (a) Cramer, C. J.; Truhlar, D. G. *Acc. Chem. Res.* **2008**, *41*, 760. (b) Mennucci, B.; Cammi, R. *Continuum Solvation Models in Chemical Physics: From Theory to Applications*; John Wiley & Sons: New York, 2007. (c) Tomasi, J.; Mennucci, B.; Cammi, R. *Chem. Rev.* **2005**, *105*, 2999. (d) Orozco, M.; Luque, F. J. *Chem. Rev.* **2000**, *100*, 4187. (e) Cramer, C. J.; Truhlar, D. G. *Chem. Rev.* **1999**, *99*, 2161.
(51) Pullman, A.; Pullman, B. *Q. Rev. Biophys.* **1975**, *7*, 505.
(52) Wesolowski, T.; Warshel, A. *J. Phys. Chem.* **1994**, *98*, 5183.
(53) Car, R.; Parrinello, M. *Phys. Rev. Lett.* **1985**, *55*, 2471.
(54) (a) Pedroza, L. S.; da Silva, A. J. R. *Phys. Rev. B* **2007**, *75*, 245331. (b) Haubein, N. C.; McMillan, S. A.; Broadbelt, L. J. *J. Chem. Inf. Comput. Sci.* **2002**, *43*, 68.
(55) (a) Gao, J. *Acc. Chem. Res.* **1996**, *29*, 298. (b) Acevedo, O.; Jorgensen, W. L. *Acc. Chem. Res.* **2009**, *43*, 142.
(56) (a) Marenich, A. V.; Ding, W. D.; Cramer, C. J.; Truhlar, D. G. *J. Phys. Chem. Lett.* **2012**, *3*, 1437. (b) Kovacs, G.; Rossin, A.; Gonsalvi, L.; Lledos, A.; Peruzzini, M. *Organometallics* **2010**, *29*, 5121. (c) Lee, M. S.; Salsbury, F. R.; Olson, M. A. *J. Comput. Chem.* **2004**, *25*, 1967.

(d) Martinez, J. M.; Pappalardo, R. R.; Marcos, E. S. *J. Phys. Chem. A* **1997**, *101*, 4444. (e) Luque, F. J.; Orozco, M. *J. Phys. Chem. B* **1997**, *101*, 5573.
(57) (a) Leszczynski, J.; Shukla, M. K. *Practical Aspects of Computational Chemistry: Methods, Concepts and Applications*; Springer: Berlin, 2010. (b) Bachrach, S. M. *Computational Organic Chemistry*; John Wiley & Sons, Inc.: New York, 2007.
(58) Rivail, J. L.; Rinaldi, D.; Ruiz-Lopez, M. F. *Liquid State Quantum Chemistry in Computational Chemistry: Review of Current Trends*; World Scientific: Singapore, 1995; p 65.
(59) Arseniyadis, S.; Valleix, A.; Wagner, A.; Mioskowski, C. *Angew. Chem., Int. Ed.* **2004**, *43*, 3314.
(60) (a) Ross, J. A.; Seiders, R. P.; Lemal, D. M. *J. Am. Chem. Soc.* **1976**, *98*, 4325. (b) Birney, D. M.; Ham, S.; Unruh, G. R. *J. Am. Chem. Soc.* **1997**, *119*, 4509. (c) Montero-Campillo, M. M.; Rodríguez-Otero, J.; Cabaleiro-Lago, E. M. *J. Phys. Chem. A* **2004**, *108*, 8373. (d) Chamorro, E.; Notario, R.; Santos, J. C.; Pérez, P. *Chem. Phys. Lett.* **2007**, *443*, 136. (e) Calvo-Losada, S.; Quirante Sánchez, J. J. *J. Phys. Chem. A* **2008**, *112*, 8164.
(61) Chen, Z.; Wannere, C. S.; Corminboeuf, C.; Puchta, R.; Schleyer, P. v. R. *Chem. Rev.* **2005**, *105*, 3842.
(62) Macchioni, A. *Chem. Rev.* **2005**, *105*, 2039.
(63) (a) Batsanov, S. S. *Inorg. Mater.* **2001**, *37*, 871. (b) Nag, S.; Banerjee, K.; Datta, D. *New J. Chem.* **2007**, *31*, 832. (c) Tatewaki, H.; Hatano, Y.; Naka, T.; Noro, T.; Yamamoto, S. *Bull. Chem. Soc. Jpn.* **2010**, *83*, 1203.
(64) (a) Belkova, N. V.; Epstein, L. M.; Shubina, E. S. *Arkivoc* **2008**, *IV*, 120. (b) Belkova, N. V.; Shubina, E. S.; Epstein, L. M. *Acc. Chem. Res.* **2005**, *38*, 624. (c) Epstein, L. M.; Shubina, E. S. *Coord. Chem. Rev.* **2002**, *231*, 165. (d) Brammer, L. *Dalton Trans.* **2003**, 3145. (e) Calhorda, M. J. *Chem. Commun.* **2000**, 801.
(65) A similar two-step profile was obtained with the 6-31G* basis set for the (C,H,N,O) atom block, although all the relative energies are systematically ca. 1 kcal/mol higher in energy; see SI for details, Figure S8.
(66) Karpfen, A. In *Advances in Chemical Physics*; John Wiley & Sons, Inc.: New York, 2003; p 469.
(67) Hammond, G. S. *J. Am. Chem. Soc.* **1955**, *77*, 334.
(68) We have located different isomers for the **ipC(s)**^{OSIP} on the PES. In some of them full loss of the C−H···Ru hydrogen-bonding interaction was detected. The corresponding geometry around the ruthenium center is almost square-planar. Representative examples are shown in Figure S10.
(69) *RT* = 0.59 kcal/mol.
(70) (*R*)-**ipE(s)**^{ISIP}: C(H)···Ru distance is 3.12 Å, angle C−H···Ru is 159°. (*S*)-**ipE(s)**^{ISIP}: C(H) ···Ru distance is 3.17 Å, angle C−H···Ru is 159°.
(71) (a) Albinati, A.; Bakhmutov, V. I.; Belkova, N. V.; Bianchini, C.; de la Rios, I. ; Epstein, L.; Gutsul, E. I.; Marvelli, L.; Peruzzini, M.; Rossi, R.; Shubina, E.; Vorontsov, E. V.; Zanobini, F. *Eur. J. Inorg. Chem.* **2002**, *2002*, 1530. (b) Shubina, E. S.; Krylov, A. N.; Belkova, N. V.; Epstein, L. M.; Borisov, A. P.; Mahaev, V. D. *J. Organomet. Chem.* **1995**, *493*, 275. (c) Shubina, E. S.; Krylov, A. N.; Kreindlin, A. Z.; Rybinskaya, M. I.; Epstein, L. M. *J. Mol. Struct.* **1993**, *301*, 1.
(72) (a) Nishio, M.; Umezawa, Y.; Suezawa, H.; Tsuboyama, S. *The Importance of Pi-Interactions in Crystal Engineering*; John Wiley & Sons, Ltd: New York, 2012; p 1. (b) Nishio, M. *Phys. Chem. Chem. Phys.* **2011**, *13*, 13873. (c) Salonen, L. M.; Ellermann, M.; Diederich, F. *Angew. Chem., Int. Ed.* **2011**, *50*, 4808. (d) Donoso-Tauda, O.; Jaque, P.; Santos, J. C. *Phys. Chem. Chem. Phys.* **2011**, *13*, 1552. (e) Takahashi, O.; Kohno, Y.; Nishio, M. *Chem. Rev.* **2010**, *110*, 6049.
(73) In general M06/SMD worked well for the geometry optimizations; however, BLYP/C-PCM performed better for the energies; see Figure S12.
(74) (*R*)-**ipE(s)**^{SSIP} can also be obtained when a scan along O−H···O$^-$ coordinate is performed for the complex (*R*)-**ipE(s)**^{ISIP}.
(75) Constrained PES scan was performed for this complex along the H−Ru coordinate in order to model the transfer of the hydrogen atom from the (*R*)-1-phenylethanol to the ruthenium atom. The scan, however, resulted in the relegation of the solvent molecule and formation of (*R*)-**ipE(s)**^{ISIP}, discussed in the text.
(76) Steiner, T.; Starikov, E. B.; Tamm, M. *J. Chem. Soc., Perkin Trans. 2* **1996**, 67.
(77) No changes in the NBO charge, however, were detected: q_H = 0.254 (cf. 0.255).
(78) Savir, Y.; Tlusty, T. *PLoS ONE* **2007**, *2*, e468.
(79) Hasanayn, F.; Morris, R. H. *Inorg. Chem.* **2012**, *51*, 10808.
(80) Zweifel, T.; Naubron, J. V.; Buttner, T.; Ott, T.; Grutzmacher, H. *Angew. Chem., Int. Ed.* **2008**, *47*, 3245.
(81) Bi, S.; Xie, Q.; Zhao, X.; Zhao, Y.; Kong, X. *J. Organomet. Chem.* **2008**, *693*, 633.
(82) Bertoli, M.; Choualeb, A.; Lough, A. J.; Moore, B.; Spasyuk, D.; Gusev, D. G. *Organometallics* **2011**, *30*, 3479.
(83) Ohkuma, T.; Utsumi, N.; Tsutsumi, K.; Murata, K.; Sandoval, C.; Noyori, R. *J. Am. Chem. Soc.* **2006**, *128*, 8724.
(84) (a) Strehlow, H.; Schneider, H. *Pure Appl. Chem.* **1971**, *25*, 327. (b) El, S. O. A. *Pure Appl. Chem.* **2007**, *79*, 1135.